On the High Frequency Asymptotic Evaluation of the Potentials of Elemental Sources on an Anisotropic Impedance Cylinder

Ronald J. Pogorzelski
Jet Propulsion Laboratory
California Institute of Technology
4800 Oak Grove Drive
Pasadena, CA 91109

Abstract - In an effort to formulate the high frequency coupling between antennas located on airframes composed of multilayer imperfectly conducting materials, a general model was sought which would embody the electromagnetic properties of the layers and would apply over a broader range of separations of the antennas. Such a model is described here. This work is a generalization of the work of pearson concerning the high frequency asymptotic representation of the fields of elemental sources diffracted by a multi layer cylinder. In that work, the source and field points were located off the cylinder surface and they were sufficiently separated to permit the effective use of the residue series representation of the spectral integrals involved. Here the source and field points are located on the cylinder surface and are permitted to be sufficiently close as to render the residue series poorly convergent. To obtain a more effective represent.ation in this situation, the cylinder is modeled by an anisotropic impedance cylinder and the resulting spectral integrals are 'evaluated by reduction to forms amenable to multiple applications of techniques described in the literature in connection with treatment of axially uniform sources in this context.

I. Introduction

As part of a study of the coupling between antennas on aircraft such as the configuration shown in Figure 1., an analytical model was constructed which consisted of a multilayer imperfectly conducting cylinder with an axially directed elemental source of either electric or magnetic type located on its outermost surface as in Figure 2. The fields of this source evaluated on the outermost surface of the cylinder are indicative of the attenuation of fields propagating on the surface and can thus

provide insight regarding the coupling to be expected between antennas located on such a cylindrical substrate. At low frequencies, of course, an eigenfunction series representation can be used to evaluate the necessary vector potentials. At high frequencies, however, such a series becomes unwieldy and a more manageable representation is sought. This usually takes the form of a residue series obtained by Watson transformation of the eigenfunction series. A general treatment of the problem using this approach was presented by Pearson [1986] [1987]. Pearson's treatment, however, required that the sources and field points be located off the surface and that they be separated sufficiently that the residue series converged reasonably rapidly. Once having obtained the residue series for the vector potentials, Pearson carried out a stationary phase integration on the axial wavenumber to obtain a solution as a sum of rays which connect the source and field points and which follow helical paths on the surface.

A similar treatment which was limited to perfectly conducting cylinders, but permitted on-surface source and field points, was carried out by Chang, et. al. [1976]. There, however, the stationary phase axial wavenumber integration was carried out first, resulting in an expression for the field components (rather than potentials) in" terms of integrals over azimuthal wavenumber which were then treated asymptotically. For large separation of source and field points, again the residue series representation was used. However, Chang et.al. extended their treatment to small separation by expanding parts of the integrands in inverse powers of the azimuthal wavenumber and recognizing the terms as known Laplace transforms. This led to a series representation in powers of the separation or Fock parameter. It is noted for future reference that this series representation is most. useful for low impedance surfaces such as the perfectly conducting one treated by Chang, et.al. If the

surface impedance is not small, the series converges very slowly unless the Fock parameter is extremely small; i.e. , the series is useful only for very small separation between source and field points. It should be noted further, however, that, while the power series applies for very small Fock parameter, it actually represents, not the true spectral integral for the field potentials but , rather, an approximation thereto. The approximation arises when one substitutes the Fock type Airy function approximation for the Hankel functions in the integrand. Since this approximation applies near the turning point of the Hankel functions, the resulting integral is not valid for arbitrarily small Fock parameter. This point will be discussed in more detail later in this exposition.

More recently, the complementary residue series / power series approach of Chang, et.al. was applied to the two dimensional problem of azimuthal rays on an impedance cylinder. [Paknys and Wang, 1987] The example calculations presented assume that the impedance parameter, q, has magnitude less than 1.0 and it is stated that when the magnitude of q is less than 1.5, the power series is useful for Fock parameters less than 0.6. Were the magnitude of q larger, the range of Fock parameters over which the power series is applicable would be considerably reduced. Thus , for high impedance surfaces, there appears a gap between the small Fock parameter range where the power series is useful and the large Fock parameter range where the residue series is useful. This intermediate range was treated many years ago by Wait [1956] and Bremmer [1958] in connection with Propagation over the surface of the earth. They were able to obtain a small curvature expansion which covered this intermediate range of Fock parameter. The first term of this expansion is mentioned by Paknys and Wang [1987] in their discussion of the planar limit. In the context of the cylinder problem treated here, the formulation of Wait and Bremmer applies only to azimuthal rays.

In this work their treatment is extended to cover the case of non-azimuthal rays (excluding only the case of purely axial propagation) .

II. Formulation

Noting that an anisotropic surface impedance cylinder can exactly model a multilayer cylinder at a fixed azimuthal mode order [D.J.Hoppe and Y. Rahmat-Samii, 1.992], we adopt the model shown in Figure 3 and select the surface impedance to match the multilayer cylinder at a mode order equal to $\beta_1 a$ where β_1 is the radial wavenumber in the exterior medium and a is the outer radius of the cylinder. This value is chosen because, in the high frequency asymptotic limit treated here, most of the contribution to the spectral integrals comes from the region of the complex order plane near $\beta_1 a$. In terms of the formulation presented by Pearson [1986], the axial magnetic and electric vector potentials for the fields on the cylinder surface due to elemental axial electric and magnetic current sources on the surface may be expressed as the spectral integral,

$$\begin{bmatrix} A \\ F \end{bmatrix} = \frac{j}{16\pi} \sum_{n=-\infty}^{\infty} \int_{-\infty}^{\infty} \int_{-\infty}^{\infty} H_\nu^{(2)}(\beta_1 a) \left\{ H_\nu^{(1)}(\beta_1 a)[I] + H_\nu^{(2)}(\beta_1 a)[R_B(\nu,\alpha)] \right\}$$

$$\times \begin{bmatrix} J \\ M \end{bmatrix} e^{-j\alpha(z-z')} \, e^{-j\nu|\phi-\phi_n'|} \, d\nu \, d\alpha \qquad (1)$$

where $\phi_n' = \phi' + 2n\pi$, $\beta_1 = \sqrt{k_1^2 - \alpha^2}$, and primed and unprimed coordinates denote the source and field points, respectively. The boundary condition on the surface of the cylinder may be

written in the form,

$$\begin{bmatrix} E_\phi \\ E_z \end{bmatrix} = \begin{bmatrix} Z_{\phi z} & Z_{\phi\phi} \\ Z_{zz} & Z_{z\phi} \end{bmatrix} \begin{bmatrix} H_z \\ H_\phi \end{bmatrix} \tag{2}$$

R_B is a two by two reflection matrix in which may be written in terms of the elements of the Z matrix as,

$$R_{B_{11}} = \left\{ \left[\frac{\Delta_z}{Z_{z\phi}} - \eta_1 L_{11} \right] \left[\frac{L_{21}}{\eta_1} + \frac{1}{Z_{z\phi}} 1 \right] - \left[\frac{\alpha\nu}{a\beta_1^2} \cdot \frac{Z_{zz}}{Z_{z\phi}} \right] \left[\frac{\alpha\nu}{a\beta_1^2} + \frac{Z_{\phi\phi}}{Z_{z\phi}} 1 \right] \right\} \frac{Q12}{\Delta} \tag{3a}$$

$$R_{B_{12}} = \left\{ \left[\frac{L_{21}}{\eta_1} - \frac{L_{11}}{\eta_1} 1 \left[\frac{\alpha\nu}{a\beta_1^2} + \frac{Z_{\phi\phi}}{Z_{z\phi}} 1 \right] \right\} \frac{Q_{12}}{} \eta_1^2 \right. \tag{3b}$$

$$R_{B_{21}} = \left\{ \left[\eta_1 L_{11} - \eta_1 L_{21} \right] \left[\frac{\alpha\nu}{a\beta_1^2} - \frac{Z_{zz}}{Z_{z\phi}} 1 \right] \right\} \frac{Q_{12}}{\eta_1^2 \Delta} \tag{3c}$$

$$R_{B_{22}} = \left\{ \left[\frac{\Delta_z}{Z_{z\phi}} - \eta_1 L_{21} \right] \left[\frac{L_{11}}{\eta_1} + \frac{1}{Z_{z\phi}} 1 \right] - \left[\frac{\alpha\nu}{a\beta_1^2} - \frac{Z_{zz}}{Z_{z\phi}} 1 \right] \left[\frac{\alpha\nu}{a\beta_1^2} + \frac{Z_{\phi\phi}}{Z_{z\phi}} 1 \right] \right\} \frac{Q_{12}}{\Delta} \tag{3d}$$

where,

$$\Delta = \left\{ \left[\frac{\Delta_z}{Z_{z\phi}} - \eta_1 L_{21} \right] H \left[\frac{L_{21}}{\eta_1} - \frac{1}{Z_{z\phi}} H + \frac{\alpha\nu}{a\beta_1^2} - \frac{Z_{zz}}{Z_{z\phi}} 1 \right] \left[\frac{\alpha\nu}{a\beta_1^2} + \frac{Z_{\phi\phi}}{Z_{z\phi}} 1 \right] \right. \tag{4}$$

$$\Delta_z = Z_{\phi z}Z_{z\phi} - Z_{\phi\phi}Z_{zz} \quad , \quad \eta_1 = \sqrt{\frac{\mu_1}{\varepsilon_1}} \quad , \tag{5}$$

$$L_{1j} = \frac{jk_j \; H_\nu^{(l)\prime}(\beta_j a)}{\beta_j \; H_\nu^{(1)}(\beta_j a)} \qquad Q_{1j}(k_1 a) = \frac{H_n^{(1)}(k_1 a)}{H_n^{(j)}(k_1 a)}, \tag{6}$$

and medium 1 is the medium exterior to the impedance cylinder. Note that this is a spectral integration over both the axial wave number, α, and the azimuthal mode number, ν. The summation on index n is the sum over multiple ray circumnavigations of the cylinder. This integral may be expanded and simplified into the forms ,

$$\mathbf{A} = \frac{j}{16\pi}\sum_{n=-\infty}^{\infty}\int_{-\infty}^{\infty}\int_{-\infty}^{\infty}\frac{4k_1}{\pi\beta_1 a}\frac{1}{\Delta}\left[L_{21} + \frac{\eta_1}{Z_{z\phi}}\right] \mathbf{J}\, e^{-j\alpha(z-z')}e^{-j\nu|\phi-\phi_n'|}d\nu\, d\alpha$$
$$+ \frac{j}{16\pi}\sum_{n=-\infty}^{\infty}\int_{-\infty}^{\infty}\int_{-\infty}^{\infty}\frac{4k_1}{\pi\beta_1 a}\frac{1}{\Delta}\left[\frac{\alpha\nu}{a\beta_1^2} + \frac{Z_{\phi\phi}}{Z_{z\phi}}\right] \mathbf{M}\, e^{-j\alpha(z-z')}e^{-j\nu|\phi-\phi_n'|}d\nu\, d\alpha \tag{7a}$$

$$\mathbf{F} = \frac{j}{16\pi}\sum_{n=-\infty}^{\infty}\int_{-\infty}^{\infty}\int_{-\infty}^{\infty}\frac{4k_1}{\pi\beta_1 a}\frac{1}{\Delta}\left[L_{21} - \frac{\Delta_z}{\eta_1 Z_{z\phi}}\right] \mathbf{M}\, e^{-j\alpha(z-z')}e^{-j\nu|\phi-\phi_n'|}d\nu\, d\alpha$$
$$+ \frac{j}{16\pi}\sum_{n=-\infty}^{\infty}\int_{-\infty}^{\infty}\int_{-\infty}^{\infty}\frac{4k_1}{\pi\beta_1 a}\frac{1}{\Delta}\left[\frac{\alpha\nu}{a\beta_1^2} - \frac{Z_{zz}}{Z_{z\phi}}\right] \mathbf{J}\, e^{-j\alpha(z-z')}e^{-j\nu|\phi-\phi_n'|}d\nu\, d\alpha \tag{7b}$$

Since the surface rays decay in amplitude exponentially for sufficiently large separation of source and field points, the n=0 term of the series will. dominate. Selecting only the n=0 term

and performing the integration on a by the method of stationary phase, results in,

$$\mathbf{A} = \frac{1}{8} e^{j\pi/4} \frac{e^{-jk_1 D}}{\sqrt{k_1 D}} \sqrt{\frac{2}{\xi}} k_1 \cos\theta \, [\mathbf{J}\, v_{11} + \mathbf{M}\, v_{12}] \tag{8a}$$

$$\mathbf{F} = \frac{1}{8} e^{j\pi/4} \frac{e^{-jk_1 D}}{\sqrt{k_1 D}} \sqrt{\frac{2}{\xi}} k_1 \cos\theta \, [\mathbf{M}\, v_{22} + \mathbf{J}\, v_{21}] \tag{8b}$$

where

$$D = \sqrt{(z-z')^2 + a^2(\phi-\phi')^2} \text{ and } \theta = \arctan\left|\frac{z-z'}{a(\phi-\phi')}\right| \tag{9}$$

$$v_{11}(\xi) = \frac{4k_1 m}{\pi\beta_1^2 a} \frac{1}{2} e^{j\pi/4} \sqrt{\frac{\xi}{\pi}} \int_{-\infty}^{\infty} \left[I_{21} + \frac{\eta_1}{Z_{z\phi}}\right] \frac{1}{\Lambda} e^{-j\xi\tau} \, d\tau \tag{10a}$$

$$v_{12}(\xi) = \frac{4k_1 m}{\pi\beta_1^2 a} \frac{1}{2} e^{j\pi/4} \sqrt{\frac{\xi}{\pi}} \int_{-\infty}^{\infty} \left[\frac{\alpha\nu}{a\beta_1^2} + \frac{Z_{\phi\phi}}{Z_{z\phi}}\right] \frac{1}{\Lambda} e^{-j\xi\tau} \, d\tau \tag{10b}$$

$$v_{21}(\xi) = \frac{4k_1 m}{\pi\beta_1^2 a} \frac{1}{2} e^{j\pi/4} \sqrt{\frac{\xi}{\pi}} \int_{-m}^{\infty} \left[\frac{\alpha\nu}{a\beta_1^2} - \frac{Z_{zz}}{Z_{z\phi}}\right] \frac{1}{\Lambda} e^{-j\xi\tau} \, d\tau \tag{10C}$$

$$v_{22}(\xi) = \frac{4k_1 m}{\pi\beta_1^2 a} \frac{1}{2} e^{j\pi/4} \sqrt{\frac{\xi}{\pi}} \int_{-m}^{\infty} \left[L_{21} - \frac{A_z}{\eta_1 Z_{z\phi}}\right] \frac{1}{\Lambda} e^{-j\xi\tau} \, d\tau \tag{10d}$$

$$m = (\beta_1 a/2)^{1/3}, \; V = m\tau + \beta_1 a, \text{ and } \xi = m|\phi - \phi'|. \tag{11}$$

The remainder of this paper deals with the asymptotic evaluation of the integrals, v_{ij} for large $\beta_1 a$ over various ranges of the Fock parameter, ξ.

III. Asymptotic Evaluation of the Integrals.

A. Review of the Azimuthal Case.

If the source and field points are at the same axial coordinate, that is z=z′, then $\theta=0$ and it follows that α, 2_{22}, and $Z_{\phi\phi}$ are also zero and $\beta_1=k_1$. In such a circumstance $v_{12}=0$, $v_{21}=0$, and,

$$v_{11}(\xi) = \frac{2}{\pi jm}\,\frac{1}{2}\,e^{j\pi/4}\sqrt{\frac{\xi}{\pi}}\int_{-\infty}^{\infty}\left[jmL_{21}-\frac{jm\Delta_z}{\eta_1 Z_{z\phi}}\right]^{-1} e^{-j\xi\tau}\,d\tau \qquad (12a)$$

$$v_{22}(\xi) = \frac{2}{\pi jm}\,\frac{1}{2}\,e^{j\pi/4}\sqrt{\frac{\xi}{\pi}}\int_{-\infty}^{\infty}\left[jmL_{21}+\frac{jm\eta_1}{Z_{z\phi}}\right]^{-1} e^{-j\xi\tau}\,d\tau \qquad (12b)$$

representing the TM and TE cases, respectively. Except for the factor $\frac{2}{\pi jm}$, these are exactly the forms treated by Paknys and Wang [1987] and by Wait [1956] and Bremmer [1958]. To see this, we note that near $\nu=k_1 a$,

$$jmL_{21} = -m\,\frac{H_\nu^{(2)\prime}(k_1 a)}{H_\nu^{(2)}(k_1 a)} \approx \frac{w_2'(\tau)}{w_2(\tau)} \qquad (13)$$

where $w_2(\tau) = \sqrt{\pi}\,[Bi(\tau) - j\,Ai(\tau)]$ and Ai and Bi are Airy functions. Recalling our earlier discussion, note that, because it applies only when $\tau \leq [2\nu/(k_1 a)]^{1/3}$ and thus is not valid for arbitrarily large τ, it is this Airy function approximation of L_{21} which invalidates the applicability of the resulting representation for arbitrarily small ξ. [Bowman, et.al., 1987, p" 57] Now, following Paknys and Wang [1987], we define

$$q = -jmC \tag{14}$$

where,

$$C = \frac{-\Delta_z}{\eta_1 Z_{z\phi}} \text{ in the TM case and,} \tag{15a}$$

$$C = \frac{\eta_1}{Z_{z\phi}} \text{ in the TE case.} \tag{15b}$$

Thus , we find that,

$$v_{ii}(\xi) = \frac{2}{\pi jm}\,\frac{1}{2}\,e^{j\pi/4}\sqrt{\frac{\xi}{\pi}}\int_{-m}^{\infty} \frac{w_2(\tau)\,e^{-j\xi\tau}}{w_2'(\tau) - qw_2(\tau)}\,d\tau = \frac{2}{\pi jm}\,v(\xi,q) \tag{16}$$

where ii=11 in the TM case and 22 in the TE case and $v(\xi,q)$ is the integral treated by Paknys and Wang [1987], Wait [1956], and Bremmer [1958].

For large values of ξ, $v(\xi,q)$ is conveniently represented as a series of residues at the poles corresponding to zeros of the denominator of the integrand; that. is, at $\tau = \tau_s$ where,

$$w_2'(\tau_s) = q\, w_2(\tau_s) \tag{17}$$

For small values of ξ, this residue series is poorly convergent and an alternative treatment. is needed. One approach is to expand the ratio $\Re$ defined below in inverse powers of τ as follows.

$$\Re = \frac{w_2'}{W_2} \sim \sqrt{\tau} - \frac{1}{4\tau} - \frac{5}{32\tau^{5/2}} - \frac{15}{64\tau^4} - \ldots \tag{18}$$

Substituting this in the integrand and expanding all but the exponential in inverse powers of τ, followed by application of Watson's lemma, results in an asymptotic representation of $v(\xi,q)$ for small ξ. As mentioned earlier, while useful for small values of q, the range of utility of this representation becomes smaller as q increases. Therefore, for large q still another treatment is needed.

The required treatment was provided by Wait [1956] and by Bremmer [1958] wherein they use the above large τ expansion of $\Re$ to show that

$$\text{R-q}^{1,} = \frac{-1}{q}\left\{ \frac{1}{1+j\sqrt{s}} - \frac{1}{2s(1+j\sqrt{s})^2}\,\delta^3 + \left[\frac{1}{4s^2(1+j\sqrt{s})^3} - \frac{5j}{8s^{5/2}(1+j\sqrt{s})^2} \right]\delta^6 + O(\delta^9) \right. \tag{19}$$

where $s = -\tau/q^2$ so that $\sqrt{s} = j\sqrt{\tau}/q$ and $\delta = (-2)^{-1/3}q^{-1}$. The terms of this expansion may now be recognized as known Laplace transforms expressible in terms of the complementary error function. That is,

$$v(\xi, q) - F(P) + \frac{1}{4 q^3} [1 - j(\pi p)^{1/2} - (1+2 P) F(P)]$$

$$+ \frac{1}{4 q^6} [1 - j(\pi p)^{1/2} (1-p) - 2p + \frac{5p^2}{6} + (p^2/2 - 1) F(P)]$$

$$+ O(q^{-9}) \qquad (20)$$

where,

$$F(p) = 1 - j(\pi p)^{1/2} e^{-p} \operatorname{erfc}(jp^{1/2}), \qquad (21)$$

and $p = j\xi q^2$ as given by Hill and Wait [1980] . This has been termed the "small curvature approximation" by virtue of the powers of δ^3 which, being inversely proportional to $\beta_1 a$, is a measure of the curvature of the surface. It is noted here that one must exercise care in the use of this formula because, strictly speaking, it represents the integral only if $\mathrm{Re}(jp^{1/2}) \geq 0$. Otherwise, one must change the algebraic sign of $p^{1/2}$ in this formula. This circumstance never arose in the work of Hill and Wait because of physical realizability constraints on the surface impedance. It will, however, arise in subsequent analysis presented here. Finally, note that this expansion is not very useful for small q owing to the increasing inverse powers of q appearing in the terms. Therefore, for small q the power series approach discussed above remains the representation of choice.

B. Treatment of the Non-azimuthal Case.

Returning to equations (10a)-(10d) , we now allow the angle, θ, to take on any value except 90 degrees corresponding to axial propagation because at 90 degrees the stationary phase

integration which led to these expressions becomes invalid. Excluding that case, we note that the denominator of the integrands of equations (10) are of the form,

$$\Delta \sim (\Re + C_1)(\Re + C_2) + (\tau + C_3)(\tau + C_4) \tag{22}$$

where the C's are independent of τ. Now, reversing the expansion (18) to obtain,

$$\tau \sim \text{!p+L+.2- -d-.o.} \quad \frac{}{2\Re} \quad \frac{}{8\Re^4} \quad \frac{}{32\Re^7} \tag{23}$$

retaining, say, two terms, and substituting this expansion into the integrands of equations (10), one finds that $\Re^2\Delta$ is a sixth degree polynomial which can be factored into the form,

$$\Re^2\Delta \sim C_o (\Re - q_1)(\Re - q_2)(\Re - q_3)(\Re - q_4)(\Re - q_5)(\Re - q_6) \tag{24}$$

Had more terms of (23) been retained, the degree of (24) would have been correspondingly higher. For example, retaining three terms leads to a twelfth degree polynomial. Specializing to v_{11}; i.e., (10a), for the moment, the corresponding numerator expression is,

$$\Re^2(D_1\Re + D_2)\ e^{-j\xi\tau} \tag{25}$$

where here the D's are independent of τ. In the case of V_{12}, the numerator is,

$$\Re^2(D_3 + D_4\tau)\ e^{-j\xi\tau} = \Re\ [\Re D_3 + D_4\ (\ \Re^3 + \frac{1}{2}\ )]\ e^{-j\xi\tau} \tag{26}$$

Thus , it becomes clear that, by partial fraction expansion, the integrands of (10) may be expressed in the form,

$$v_{ij} \sim \sum_{n=1}^{6} \int_{-\infty}^{\infty} \frac{A_n}{(\Re - q_n)} e^{-j\xi\tau} \, d\tau \tag{27}$$

The six integrals in (27) are now of the form (16) and can therefore be treated asymptotically in the same manner. Thus , treatment of the case of general θ has been reduced to repeated application of the methods used in the azimuthal case, θ=0. Note that in carrying out this prescription," if only two terms are retained in (23) , one is justified in retaining only, two terms in (20) resulting in what will be termed a "two term small curvature approximation." If, however, three terms are retained in (23), one is then justified in including three terms in (20) leading to a "three term small curvature approximation."

It is noted in passing that one need not necessarily approximate the numerator (26) with the series (23) . An alternative procedure would be to leave the numerator in the form,

$$\Re^2(D_3 + D_4\tau) \, e^{-j\xi\tau} \tag{28}$$

and produce a partial fraction expansion leading to,

$$v_{ij} \sim \sum_{n=1}^{6} \int_{-\infty}^{\infty} \frac{A_n + B_n\tau}{(\Re - q_n)} e^{-j\xi\tau} \, d\tau \tag{29}$$

Then, the A_n terms can be approximated as in the azimuthal case while the B_n terms can be approximated by differentiating the results for the A_n terms with respect to $-j\xi$. This, in fact, is the method used in the examples to follow.

IV. Illustrative Numerical Examples.

To illustrate the ranges of applicability of the various representations described above, two example cylindrical geometries were chosen. Each is a circular cylinder with a one tenth free space wavelength thick dielectric coating. The dielectric has a complex relative permittivity of 6.65-j3.00 and the permeability of free space. The electrical outer radius, $k_1 a$, of the coated cylinder is 12 in one case and 500 in the other where k_1 is the wavenumber of the exterior medium; i.e., free space. These two radii demonstrate the representations both in the large radius regime where they are most accurate and for a small radius where their accuracy deteriorates somewhat due primarily to the inaccuracy of the Fock type Airy function approximation of the Hankel functions. These cylinders were then approximated by impedance cylinders of the same outer radii where the anisotropic surface impedances "were determined by matching the modal reflection coefficients at mode order $\nu = \beta_1 a$. (This, of course, means that the impedances are dependent on the angle of ray propagation on the surface.)

We begin by reproducing the results for the azimuthal case to validate the computations. Consider the magnitude and phase of the Fock integrals, v_{1j}, for the larger cylinder in the azimuthal case. Figure 4, shows both the four term residue series result and that of the three term small curvature approximation of Wait and Bremmer for the TM polarization. The poles and residues were computed from the unapproximated integrands for the impedance cylinder while the small curvature approximation, of course, involved the approximation of the Hankel function by the Fock type Airy functions. This will be the case unless otherwise noted. (Note that the label "90 degree path" refers to the complement of the angle θ. This convention is used throughout

the set of examples presented here.) A smooth transition from one approximation to the other may be observed in the vicinity of ξ=0.6. Similar behavior is shown in Figure 5 for the TE polarization. Figure 6 compares the small curvature approximation of Figure 5 with the power series expansion for small ξ. Both are based on the integrand with Hankel functions approximated with Fock type Airy functions. Note that, because of the large magnitude of q (i.e., nearly 6) , the power series fails for ξ greater than about 0.03 whereas for q on the order of unity, Paknys and Wang showed good results up to ξ=0.6. Thus, in the subsequent examples, the power series is used for q's of magnitude less than or equal. to unity and the small curvature approximation is used for q's of magnitude greater than unity.

Moving now to a 45 degree ray path, Figures 7a, 7b, and 7c illustrate the results for the three Fock integrals, v_{11}, v_{12}, and V_{22}. (Recall that $v_{21} = v_{12}$.) Here eight residue terms are used to obtain the same order of approximation as with four terms in the azimuthal case because here both polarizations are involved. Corresponding results using the two term small curvature approximat.ion are shown in Figures 8a, 8b, and 8c. The deterioration of the approximation is quite evident. In fact, it would be difficult to determine from the two term approximation the proper value of the Fock parameter at which to make the transition between the two approximations. The three term approximation in Figure 7 makes it clear that the proper transition is in the vicinity of ξ=0.65.

To explore the low frequency limitations of the high frequency asymptotic approximations, the above computations were repeated for the small cylinder; i.e., for k_1a=12. The results for the two term small curvature approximation are shown in Figures 9a, 9b, and 9c while the three term results are shown in Figures 10a, 10b, and 10c. While the three term approximation provides some

improvement, in neither set of curves is there a clearly defined smooth transition between the small and large Fock parameter representations, particularly in the case of the magnitude. The addition of more terms extends the residue series validity to lower values of Fock parameter as shown in Figures ha, 11b, and 11c. Nevertheless, the transition to the small curvature approximation is still not very clearly defined. Recall now that that the residue series are derived from the exact integrands. If, instead, one uses the poles and residues of the integrands in which the Hankel functions have been approximated by Fock type Airy functions, that is, the integrands used in the small curvature approximation, one finds a much better defined transition as shown in Figures 12a, 12b, and 12c. From this one may conclude that the deterioration observed as the electrical size of the cylinder decreases is not primarily due to deterioration in either the residue series or the small curvature approximation. Rather, it is primarily due to deterioration of the approximation of the Hankel functions by Fock type Airy functions as in (13). One might try to improve the low frequency validity of this treatment by adding more terms to this asymptotic approximation. Such terms may be obtained from the expansion given by Bowman, Senior, and Uslenghi [1987]. While this is deemed beyond the scope of the present treatment, the next order terms of the necessary approximation (proportional to m^{-2}) are given below for reference.

$$imL_{21} = -m \frac{H_\nu^{(2)'}(k_1 a)}{H_\nu^{(2)}(k_1 a)} \approx \Re + \frac{1}{60m}(4\tau+\tau^2)\Re + \frac{1}{600m^2}(6+4\tau-\tau^3)$$

Here again τ is to be replaced by (23). While it is not rigorously guaranteed that addition of these terms will improve the accuracy of the approximation, this expression may be used to estimate the impact of truncation at one term in a given situation. For example, for the case of purely azimuthal rays on

the cylinder of ka=500 in Figures 4,5, and 6, the first and second terms of this expansion are roughly equal in magnitude for ξ=0.075 indicating that, for Fock parameter values below this, the first term of the approximation is probably inadequate. Finally, it is noted that, regardless of how many terms of this approximation are retained, the resulting integrands will not be valid for arbitrarily large τ. Therefore, the asymptotic approximation of the integrals will not extend to arbitrarily small ξ. To extend the approximation to arbitrarily small ξ, one should expand the *exact* integrands in inverse powers of τ in analogy with the treatment of Paknys and Wang. (Recall that they expanded the ***approximate*** integrand.) This, too, is deemed beyond the scope of the present treatment.

Studies similar to the above have been carried out for ray paths at angles of 30 degrees and 60 degrees with results very similar in character to those presented here. While it is recognized that these approximations will not. be valid for purely axial ray paths and will deteriorate in accuracy near axial propagation, these studies indicate that the approximation techniques presented are valid and useful for all ether angles.

V. Concluding Summary.

In this work the small curvature expansion of Wait and Bremmer has been generalized to the case of non-azimuthal rays. This provides a high frequency asymptotic approximation of the coupling between antennas located on an impedance cylinder when their separation is too small for effective use of the usual residue series. The result is applicable to the problem of estimating the coupling between antennas mounted on non-perfectly conducting aircraft skins. Example calculations are presented for both the azimuthal ray case (for validation purposes) and the

general case (excluding axial propagation). These examples demonstrate that the approximation complements the residue series and power series approximations in the intermediate range of Fock parameter.

VI. Acknowledgements.

Stimulating and inspiring discussions with Dr. Paul Hussar of Illinois Institute of Technology Research Institute, with Professor Yahya Rahmat-Samii of the University of California at Los Angeles, and especially with Professor James R. Wait of the University of Arizona are gratefully acknowledged. Thanks are also due Professor L. Wilson Pearson of Clemson University for the use of a computer code he developed while at McDonnell Douglas Research LaboratoriesAan augmented version of which was used to locate the poles “and compute the residues of the integrands of the spectral integrals.

Parts of this research were carried out at the Jet Propulsion Laboratory, California Institute of Technology, under contract with the National Aeronautics and Space Administration.

References

Bowman, J. J., T. B. A. Senior, and P. L. E. Uslenghi (1987), Electromagnetic and Acoustic Scattering by Simple Shapes, Hemisphere.

Bremmer, H. (1958), Applications of Operational Calculus to Ground-Wave Propagation, Particularly for Long Waves, IRE Trans. Antennas Propagat. , pp. 267-272.

Chang, Z. W., L. B. Felsen, and A. Hessel (1.976), Surface Ray Methods for Mutual Coupling in Conformal Arrays on Cylindrical and Conical Surfaces, Final Report on U. S. Navy Contract NO0123-76-C-0236, AD--AO33544.

Hill, D. A. and J. R. Wait (1980), Ground Wave Attenuation Function for a Spherical Earth with Arbitrary Surface Impedance, Radio Science, 15(3), 637-643.

Hoppe, D. J. and Y. Rahmat-Samii (1992) , Scattering by Superquadric Dielectric-Coated Cylinders using Higher Order Boundary Conditions, IEEE Trans. Antennas Propagat. , AP-40(12), 1513-1523.

Paknys, R. and N. Wang (1987) , High-Frequency Surface Field Excited by a Magnetic Line Source on an Impedance Cylinder, IEEE Trans. Antennas Propagat. , AP-35(3) , 293-298.

Pearson, L. W. (1986), A Construction of the Fields Radiated by z-Directed Point Sources on Current in the Presence of a Cylindrically Layered Obstacle, Radio Science, 21(4), 559-569.

Pearson, L. W. (1987) , A Ray Representation of Surface Diffraction by a Multilayer Cylinder, IEEE Trans. Antennas Propagat. , AP-35(6), 698-707.

Wait, J. R. (1956), Radiation from a Vertical Antenna over a Curved Stratified Ground, J. of Res. of NBS, 56(4), 237-244.

Figure Captions

Figure 1. Ray paths for coupling between antennas on an airframe.

Figure 2. Multilayer cylinder model of aircraft skin.

Figure 3. Impedance cylinder model.

Figure 4. Asymptotic representations for azimuthal rays in the TM case.

Figure 5. Asymptotic representations for azimuthal rays in the TE case.

Figure 6. Comparison of small curvature and power series representations for azimuthal rays in the TE case.

Figure 7a. Asymptotic representations for helical ray path in TM-TM coupling; three term small curvature approximation.

Figure 7b. Asymptotic representations for helical ray path in TM-TE coupling three term small curvature approximation.

Figure 7c. Asymptotic representations for helical ray path in TE-TE coupling three term small curvature approximation.

Figure 8a. Asymptotic representations for helical ray path in TM-TM coupling; two term small curvature approximation.

Figure 8b. Asymptotic representations for helical ray path in TM-TE coupling two term small curvature approximation.

Figure 8c. Asymptotic representations for helical ray path in TE-TE coupling two term small curvature approximation.

Figure 9a. Asymptotic representations for helical ray path in TM-TM coupling on a small cylinder using a two term small curvature approximation.

Figure 9b. Asymptotic representations for helical ray path in TM-TE coupling on a small cylinder using a two term small curvature approximation.

Figure 9c. Asymptotic representations for helical ray path in TE-TE coupling on a small cylinder using a two term small curvature approximation.

Figure lOa. Asymptotic representations for helical ray path in TM-TM coupling on a small cylinder using a three. term small curvature approximation.

Figure 10b. Asymptotic representations for helical ray path in TM-TE coupling on a small cylinder using a three term small curvature approximation.

Figure 10c. Asymptotic representations for helical. ray path in TE-TE coupling on a small cylinder using a three term small curvature approximation.

Figure ha. Asymptotic representations for helical ray path in TM-TM coupling on a small cylinder using a sixteen term residue series.

Figure 11b. Asymptotic representations for helical ray path in TM-TE coupling on a small cylinder using a sixteen term residue series.

Figure 11c. Asymptotic representations for helical ray path in TE-TE coupling on a small cylinder using a sixteen term residue series.

Figure 12a. Asymptotic representations for helical ray path in TM-TM coupling on a small cylinder using a ten residues of the Fock approximation.

Figure 12b. Asymptotic representations for helical ray path in TM-TE coupling on a small cylinder using a ten residues of the Fock approximation.

Figure 12c. Asymptotic representations for helical ray path in TE-TE coupling on a small cylinder using a ten residues of the Fock approximation.

ANTENNA COUPLING ON AN AIRFRAME

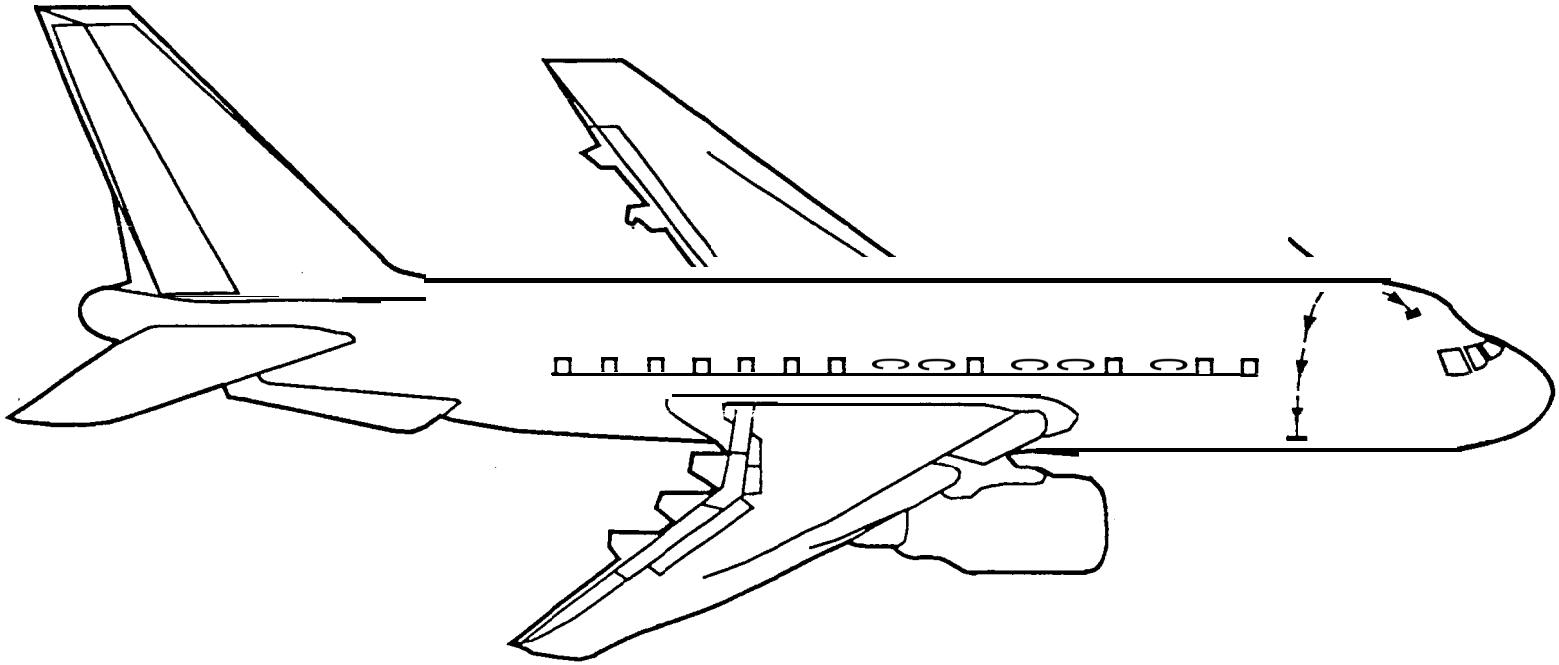

FIG.

COUPLING GEOMETRY

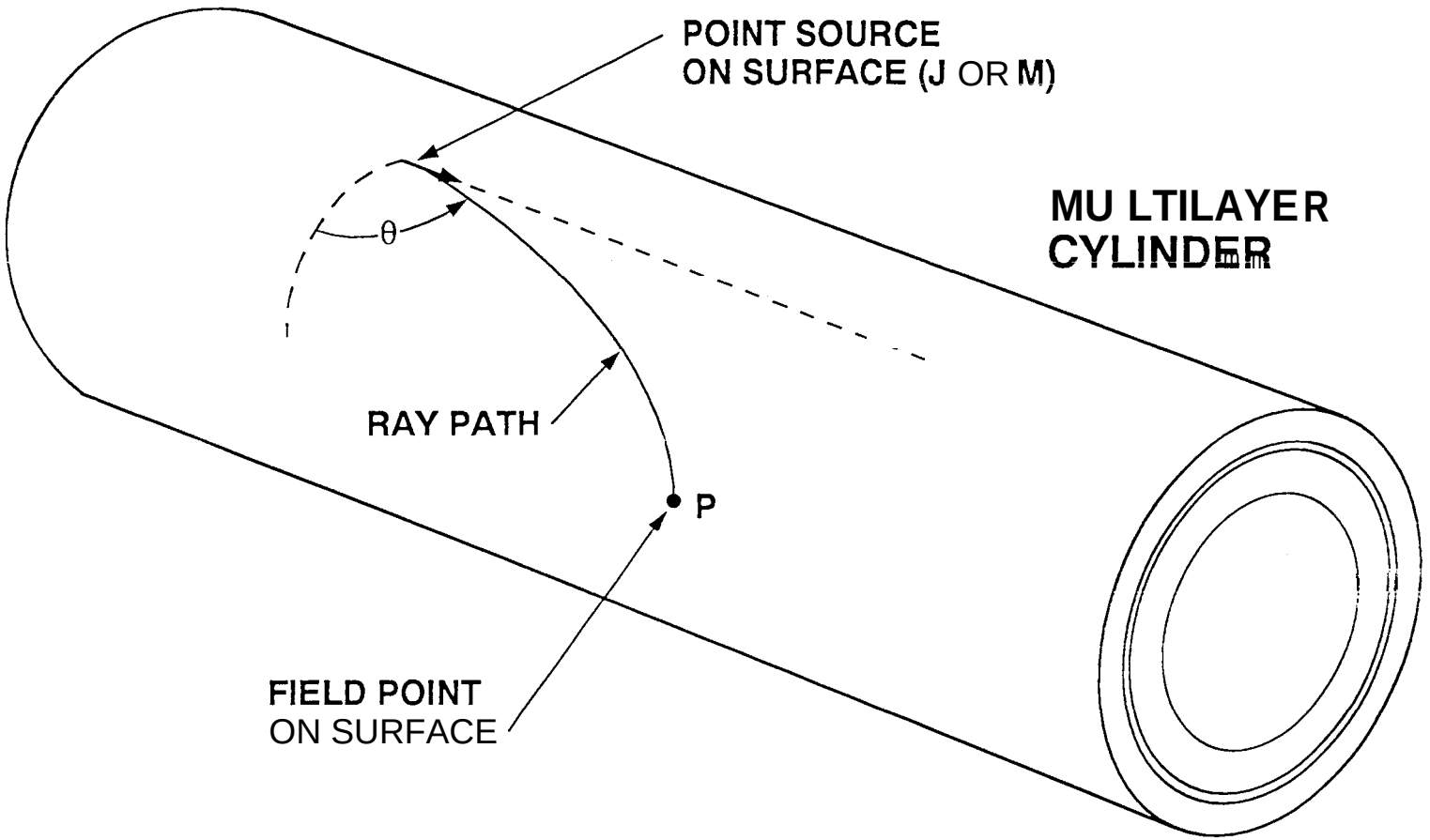

FIG. 2

SURFACE IMPEDANCE MODEL

$$\begin{bmatrix} E_\phi \\ E_z \end{bmatrix} = \begin{bmatrix} Z_{\phi z} & Z_{\phi\phi} \\ Z_{zz} & Z_{z\phi} \end{bmatrix} \begin{bmatrix} H_z \\ H_\phi \end{bmatrix}$$

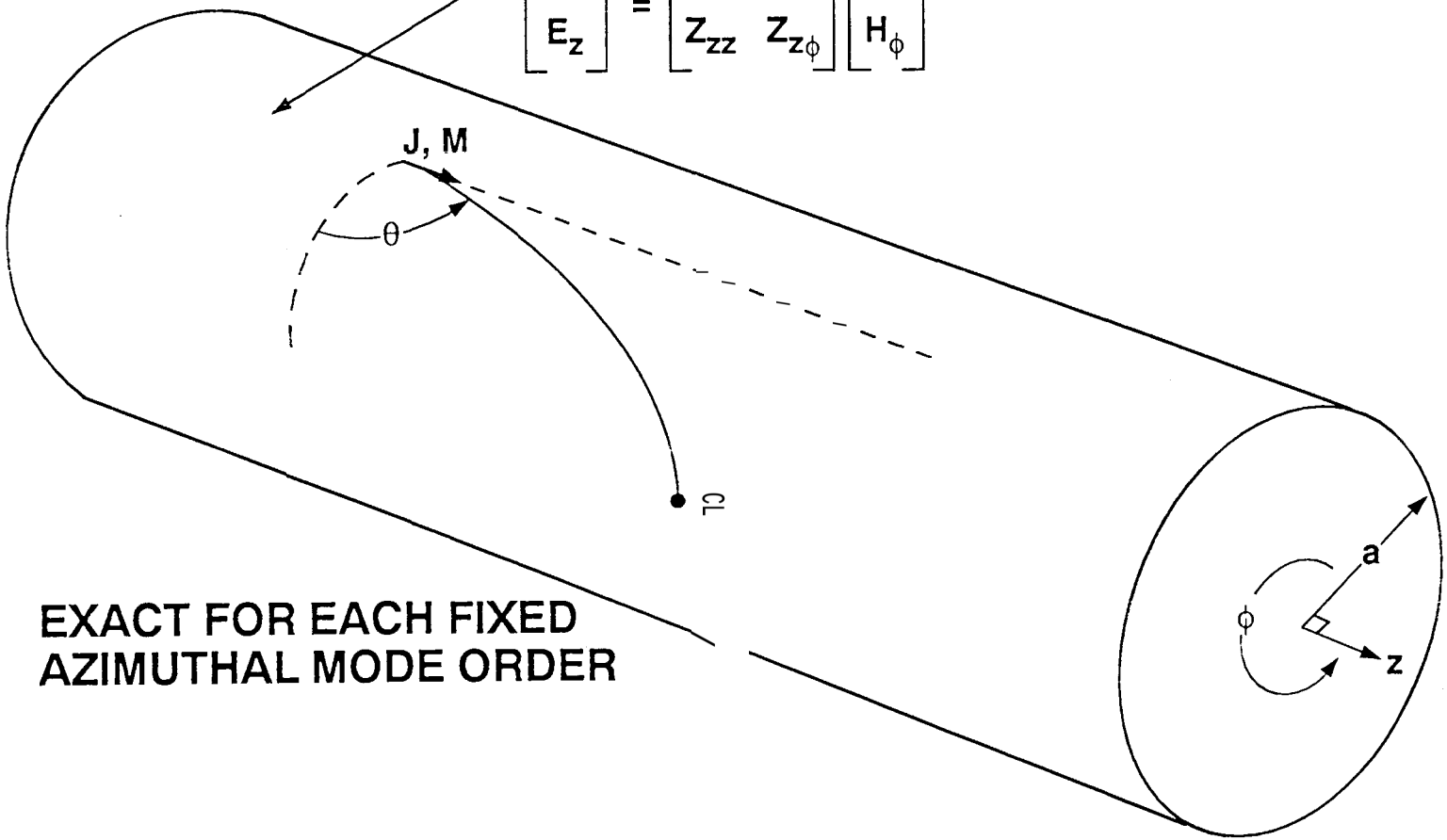

EXACT FOR EACH FIXED
AZIMUTHAL MODE ORDER

ASYMPTOTIC REPRESENTATIONS

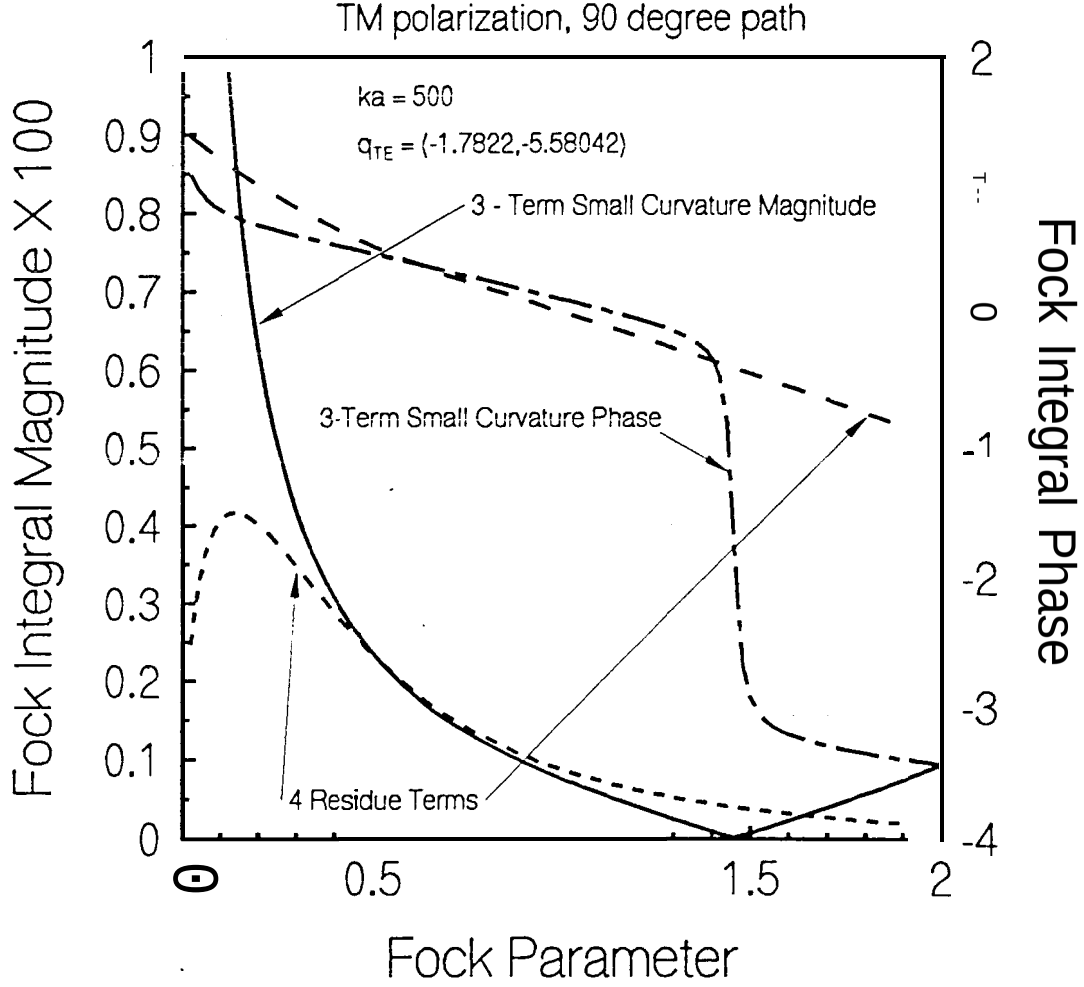

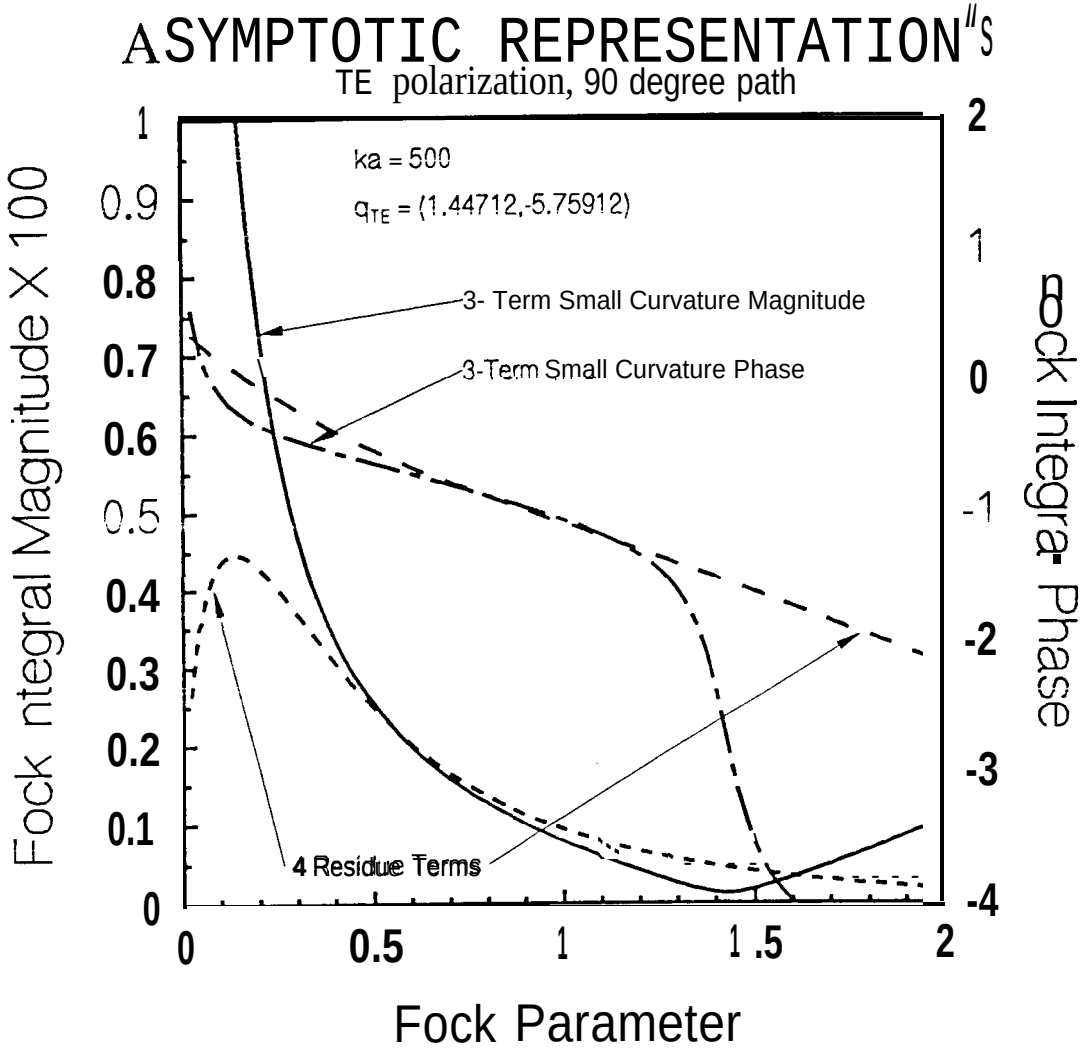
ASYMPTOTIC REPRESENTATION"S
TE polarization, 90 degree path
ka = 500
q_{TE} = (1.44712,-5.75912)
3- Term Small Curvature Magnitude
3-Term Small Curvature Phase
4 Residue Terms
Fock ntegral Magnitude X 100
ock Integra- Phase
Fock Parameter
1
0.9
0.8
0.7
0.6
0.5
0.4
0.3
0.2
0.1
0
2
1
0
-1
-2
-3
-4
0
0.5
1
1 .5
2

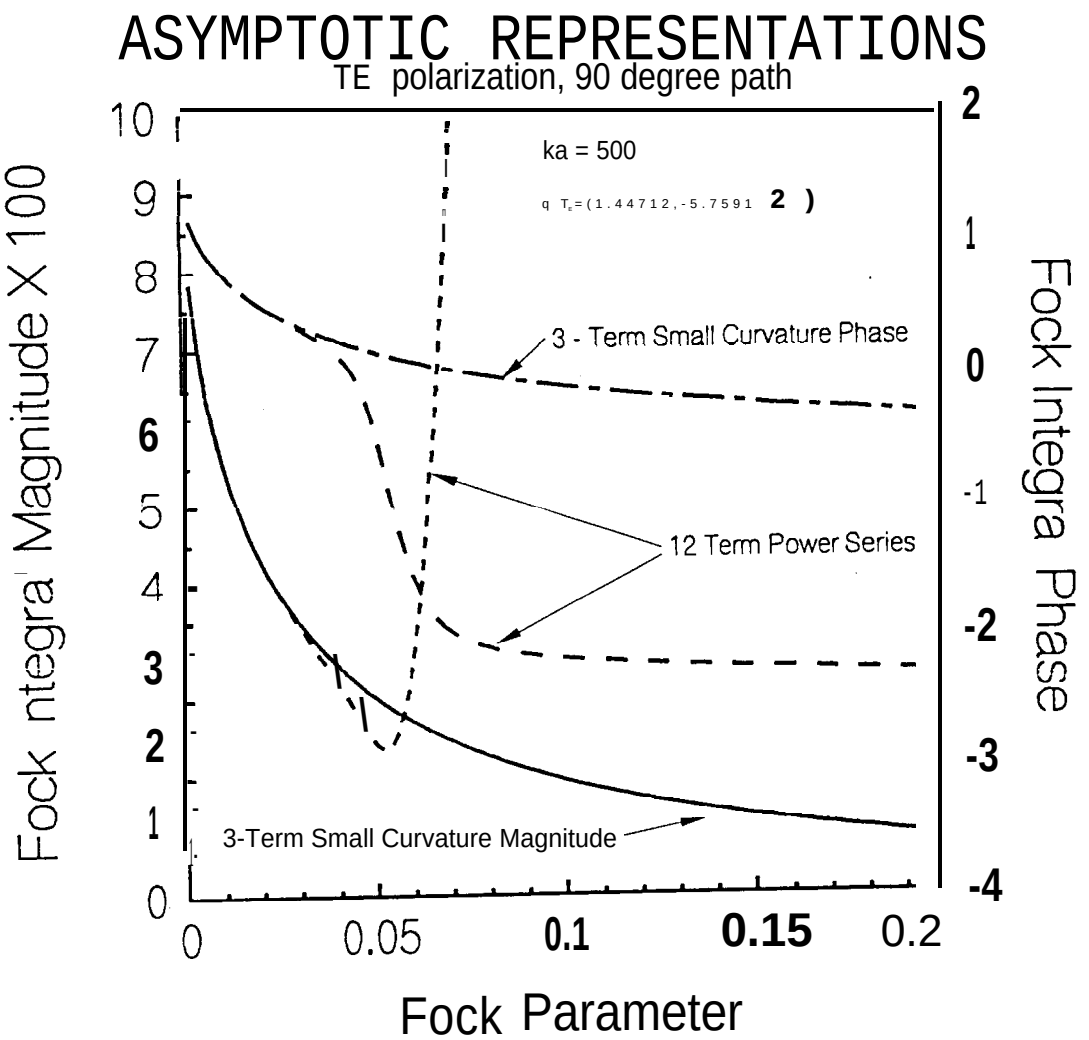
ASYMPTOTIC REPRESENTATIONS
TE polarization, 90 degree path
ka = 500
q Te=(1.44712,-5.7591 2)
3 - Term Small Curvature Phase
12 Term Power Series
3-Term Small Curvature Magnitude
Fock ntegra Magnitude X 100
Fock Integra Phase
Fock Parameter
10
9
8
7
6
5
4
3
2
1
0
2
1
0
-1
-2
-3
-4
0
0.05
0.1
0.15
0.2

FIG. 6

ASYMPTOTIC REPRESENTATIONS

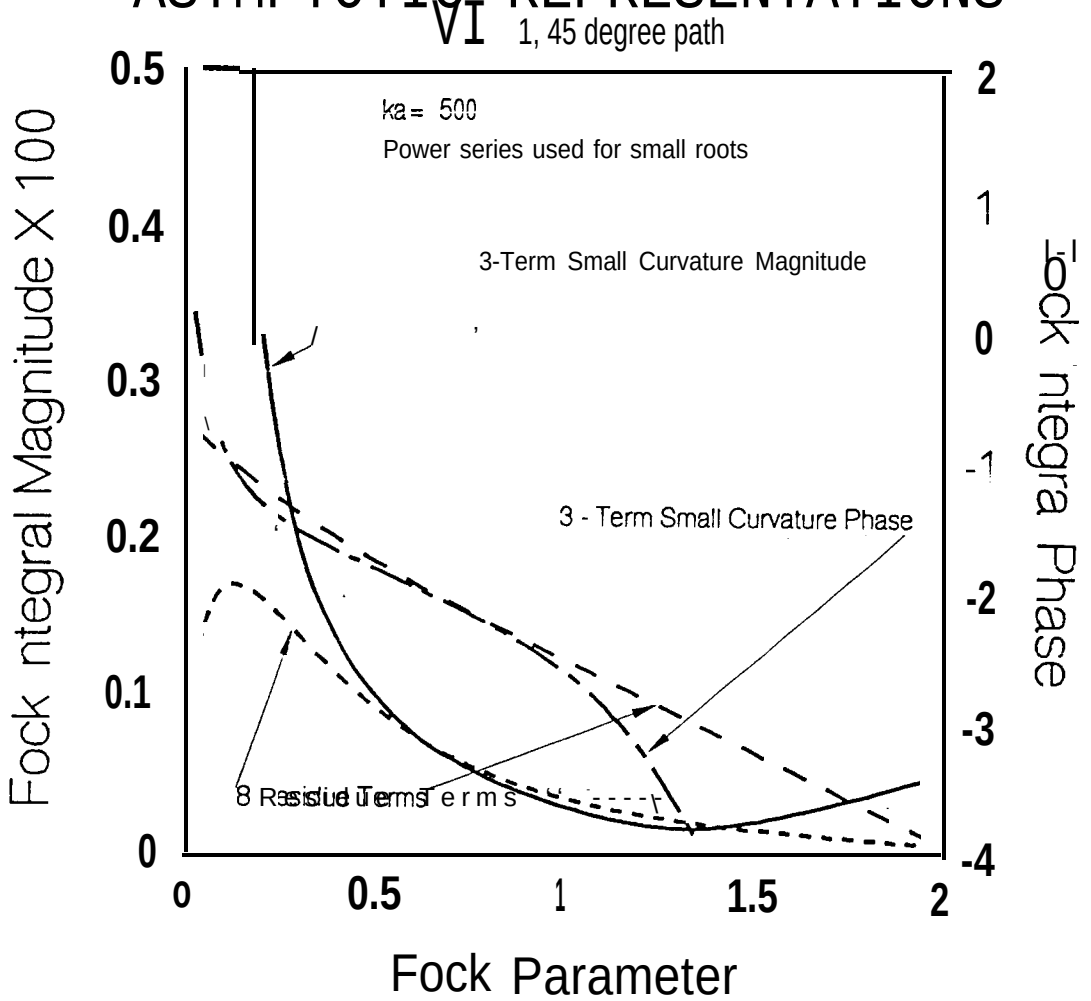

FIG. 7a

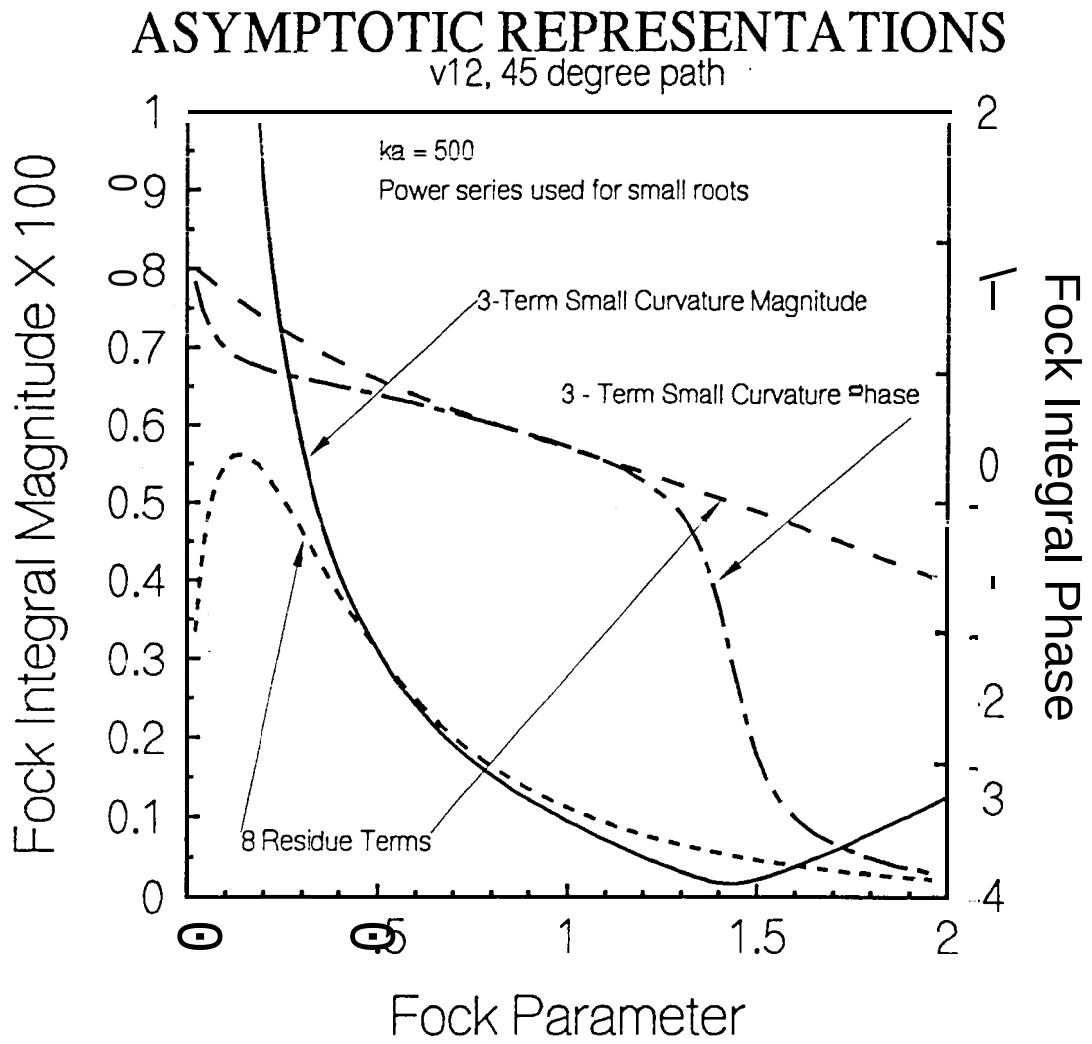
ASYMPTOTIC REPRESENTATIONS
v12, 45 degree path
ka = 500
Power series used for small roots
3-Term Small Curvature Magnitude
3 - Term Small Curvature Phase
8 Residue Terms
Fock Integral Magnitude X 100
Fock Integral Phase
Fock Parameter
0
0.1
0.2
0.3
0.4
0.5
0.6
0.7
0.8
0.9
1
0
0.5
1
1.5
2
-1
-2
-3
-4

FIG. 7b

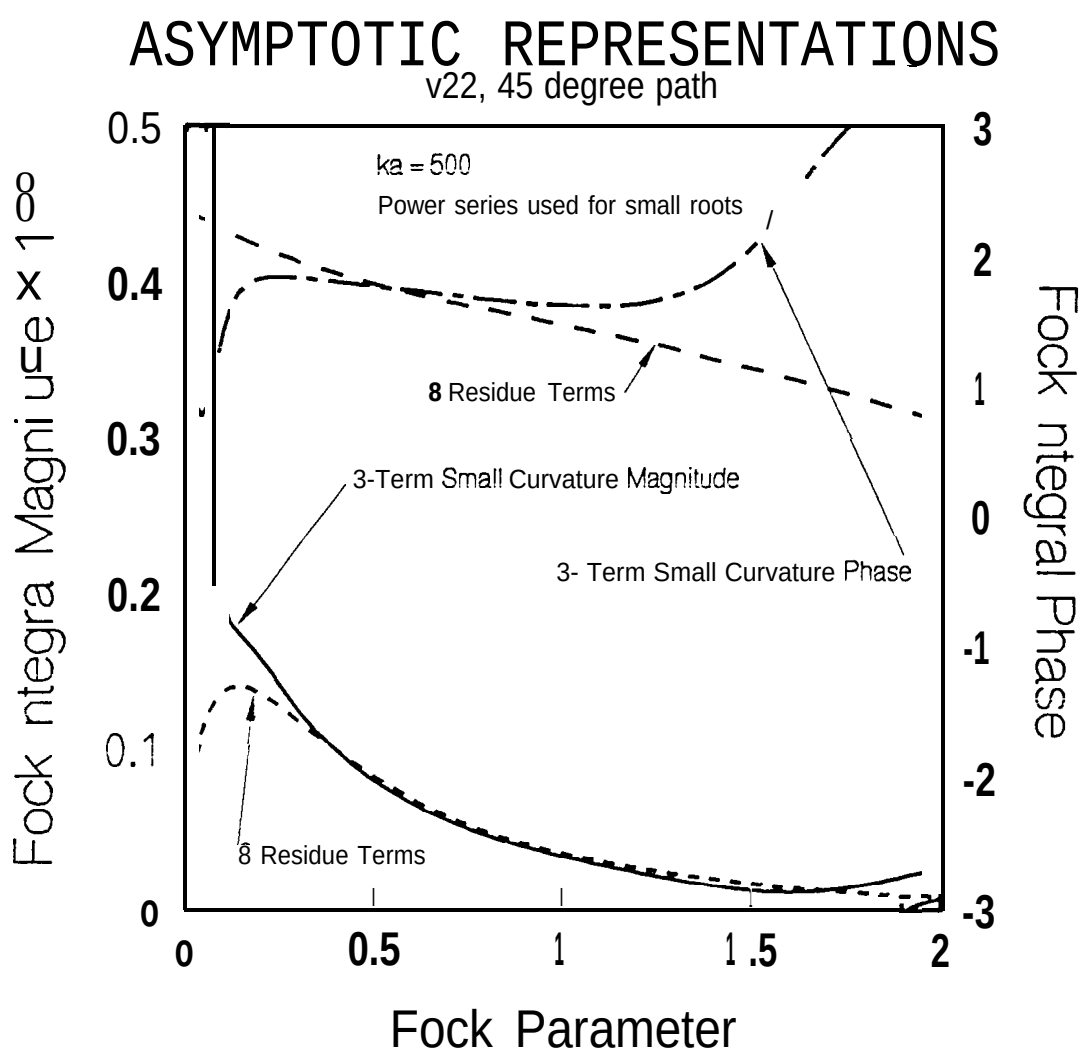
ASYMPTOTIC REPRESENTATIONS
v22, 45 degree path
ka = 500
Power series used for small roots
8 Residue Terms
3-Term Small Curvature Magnitude
3- Term Small Curvature Phase
8 Residue Terms
Fock ntegra Magni uce x 1 8
Fock ntegral Phase
Fock Parameter
0.5
0.4
0.3
0.2
0.1
0
3
2
1
0
-1
-2
-3
0
0.5
1
1.5
2

FIG. 7c

ASYMPTOTIC REPRESENTATIONS

VI 1, 45 degree path .

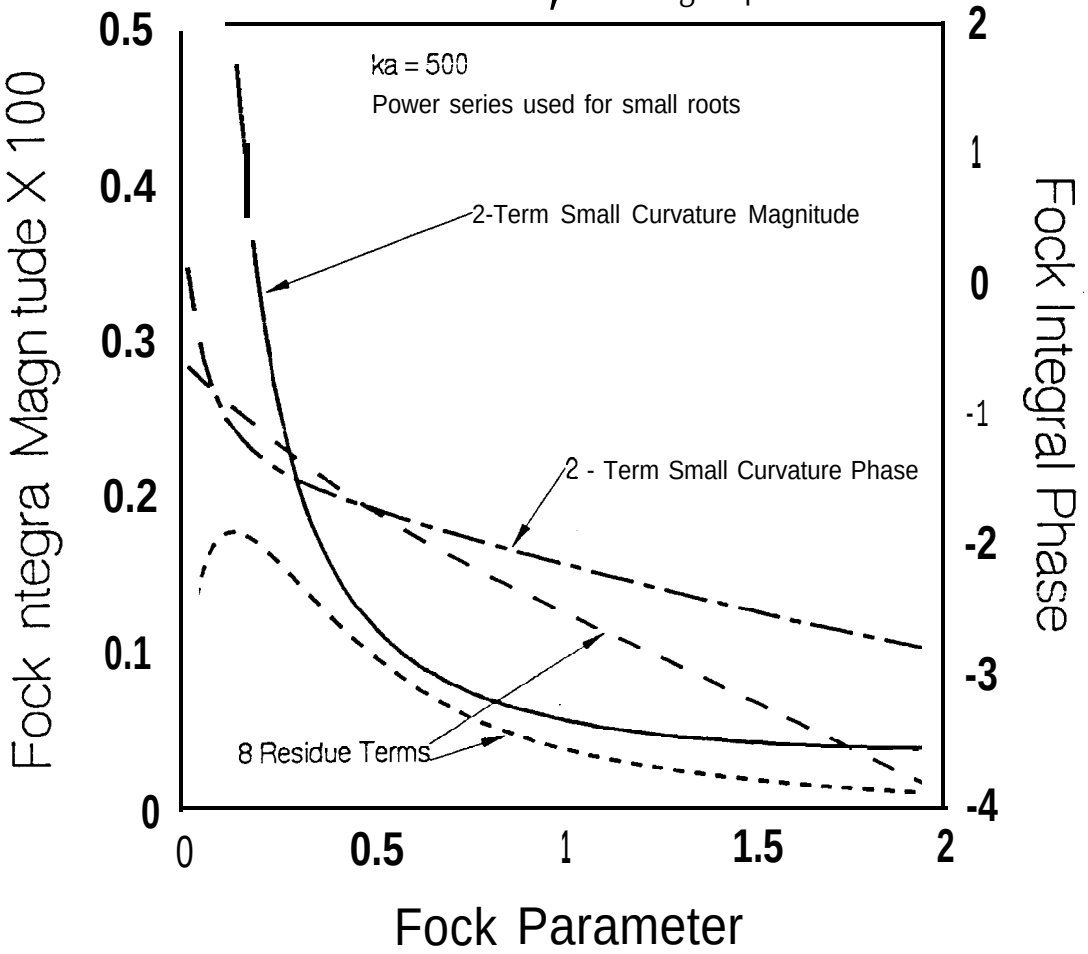

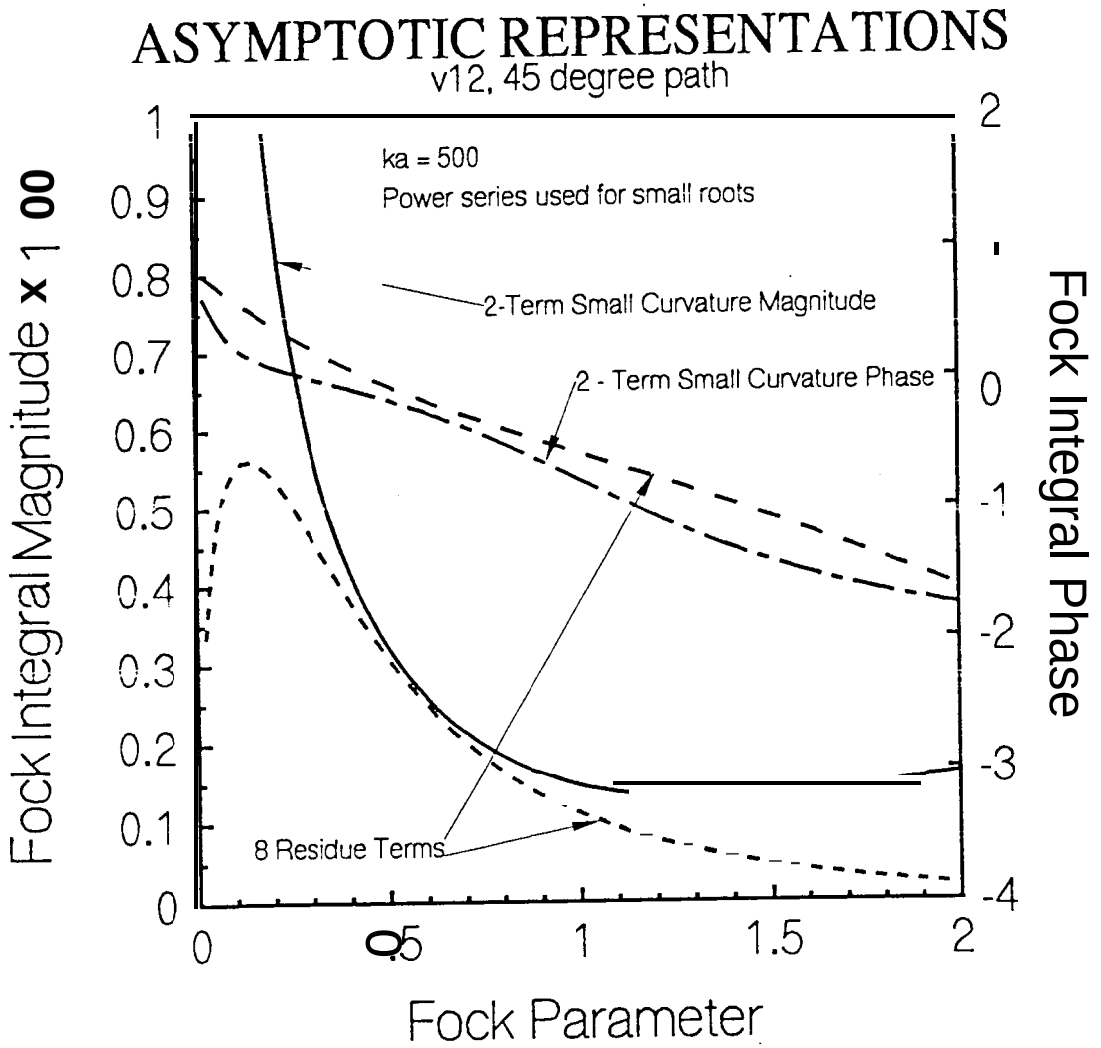
ASYMPTOTIC REPRESENTATIONS
v12, 45 degree path
ka = 500
Power series used for small roots
2-Term Small Curvature Magnitude
2 - Term Small Curvature Phase
8 Residue Terms
Fock Integral Magnitude x 1 00
Fock Integral Phase
Fock Parameter
1
0.9
0.8
0.7
0.6
0.5
0.4
0.3
0.2
0.1
0
2
0
-1
-2
-3
-4
0
Q.5
1
1.5
2

ASYMPTOTIC REPRESENTATIONS

v22, 45 degree path

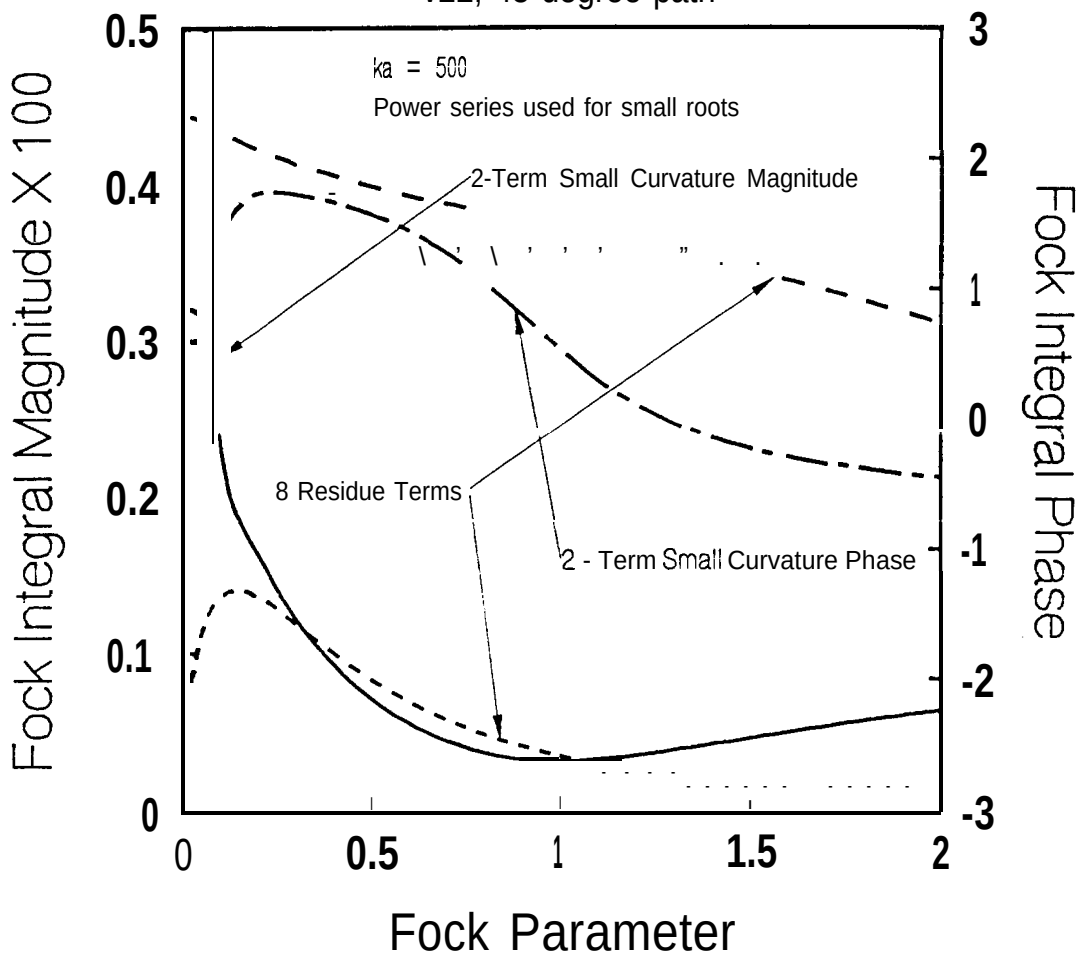

ASYMPTOTIC REPRESENTATIONS

VI 1, 45 degree path

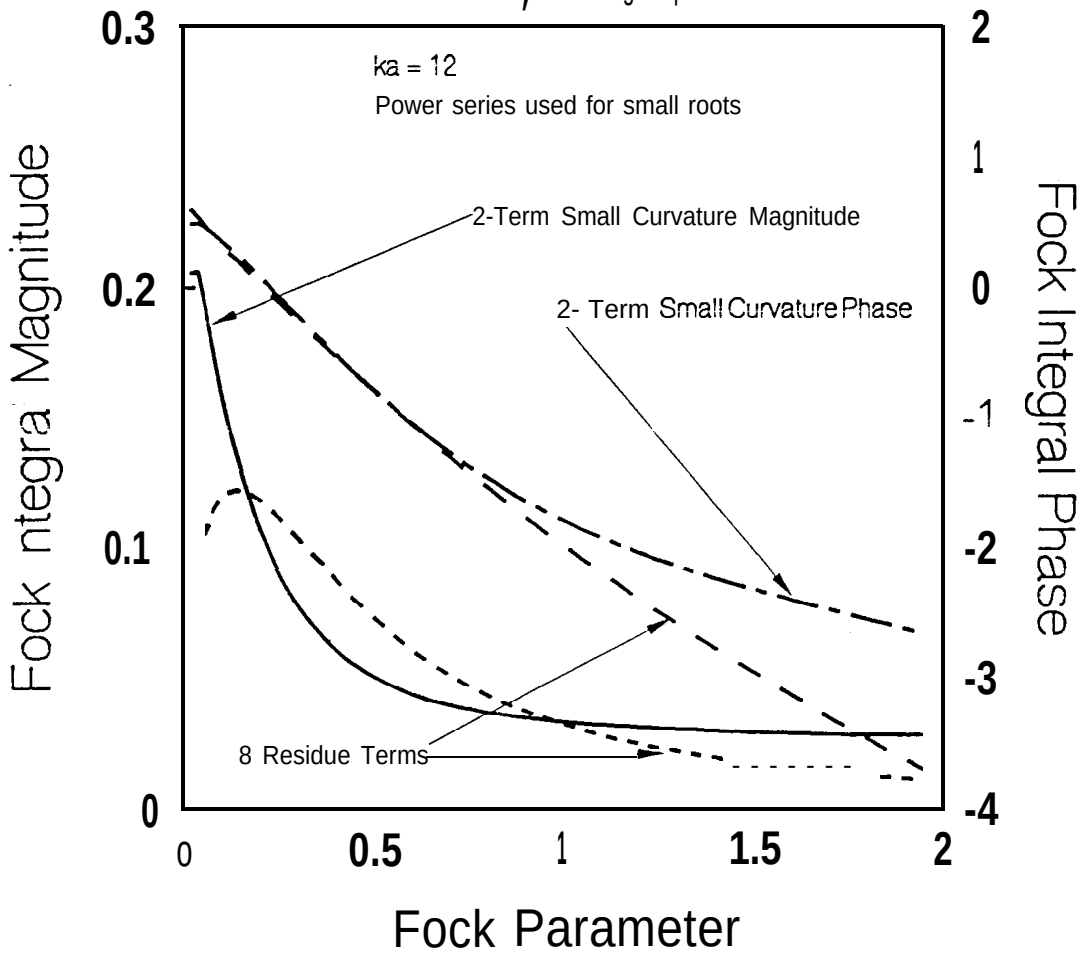

FIG. 99

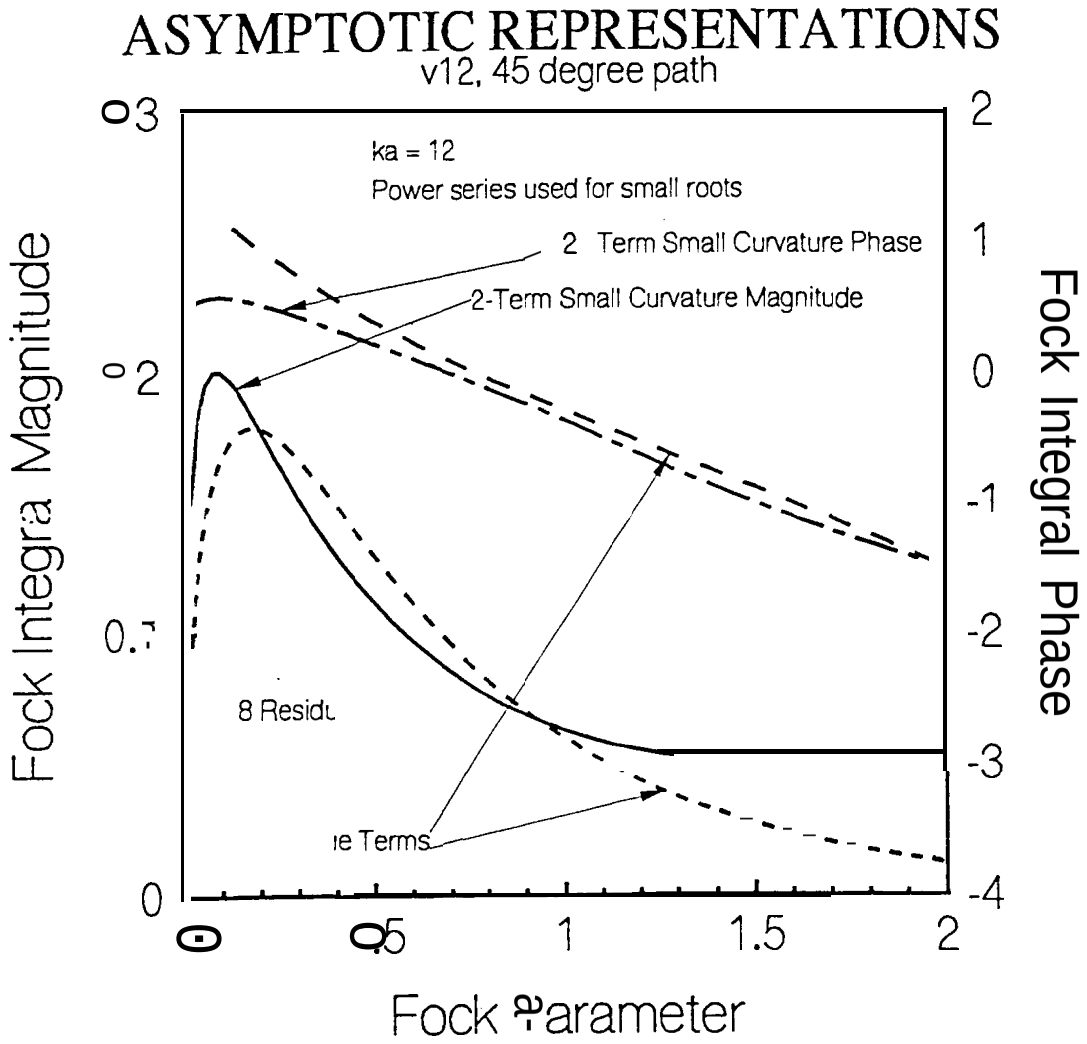
ASYMPTOTIC REPRESENTATIONS
v12, 45 degree path
ka = 12
Power series used for small roots
2 Term Small Curvature Phase
2-Term Small Curvature Magnitude
8 Residu
ıe Terms
Fock Integra Magnitude
Fock Integral Phase
Fock ɐarameter
0
0.5
1
1.5
2
-1
-2
-3
-4

FIG. 96

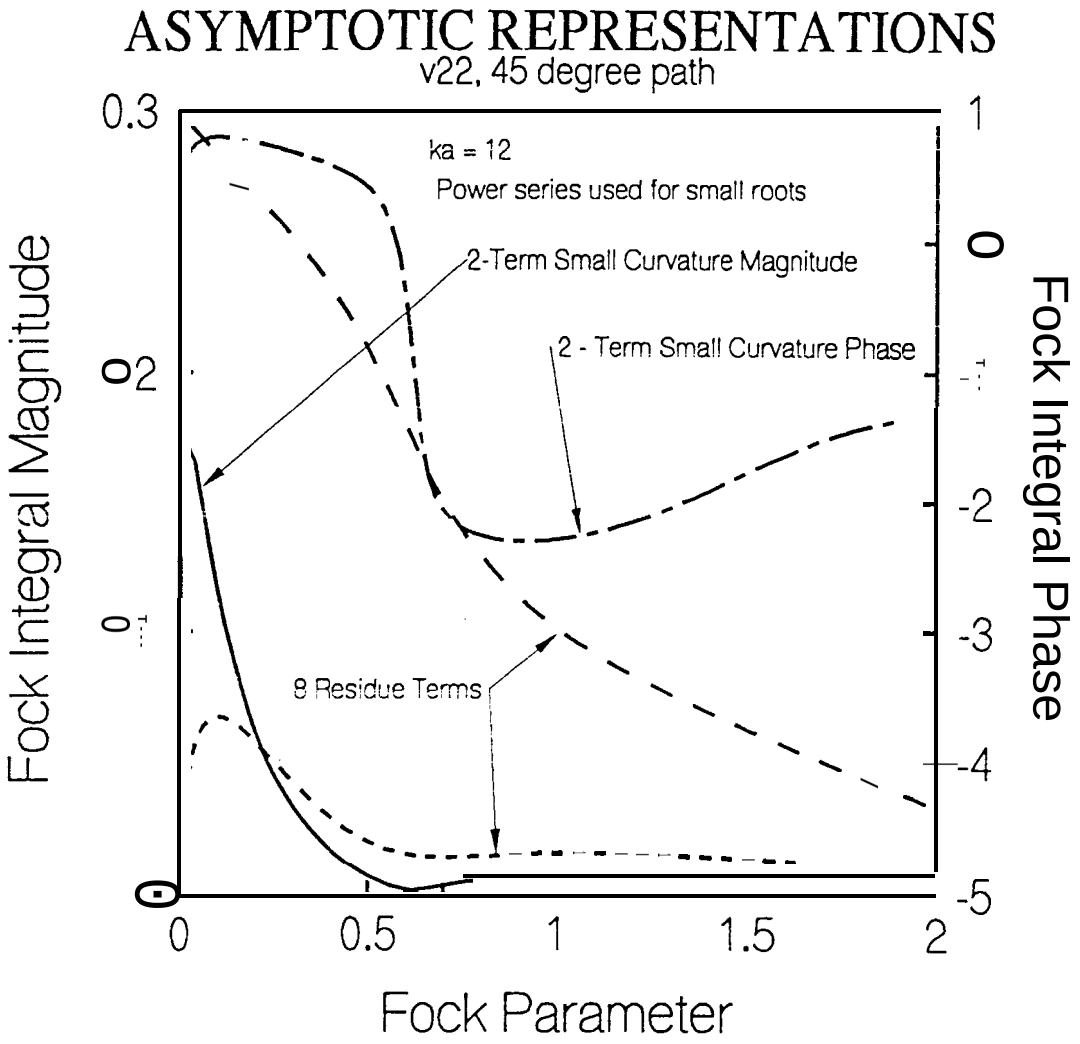
ASYMPTOTIC REPRESENTATIONS
v22, 45 degree path
ka = 12
Power series used for small roots
2-Term Small Curvature Magnitude
2 - Term Small Curvature Phase
8 Residue Terms
Fock Integral Magnitude
Fock Integral Phase
Fock Parameter
0.3
0.2
0.1
0
1
0
-1
-2
-3
-4
-5
0
0.5
1
1.5
2

FIG. 9C

ASYMPTOTIC REPRESENTATIONS

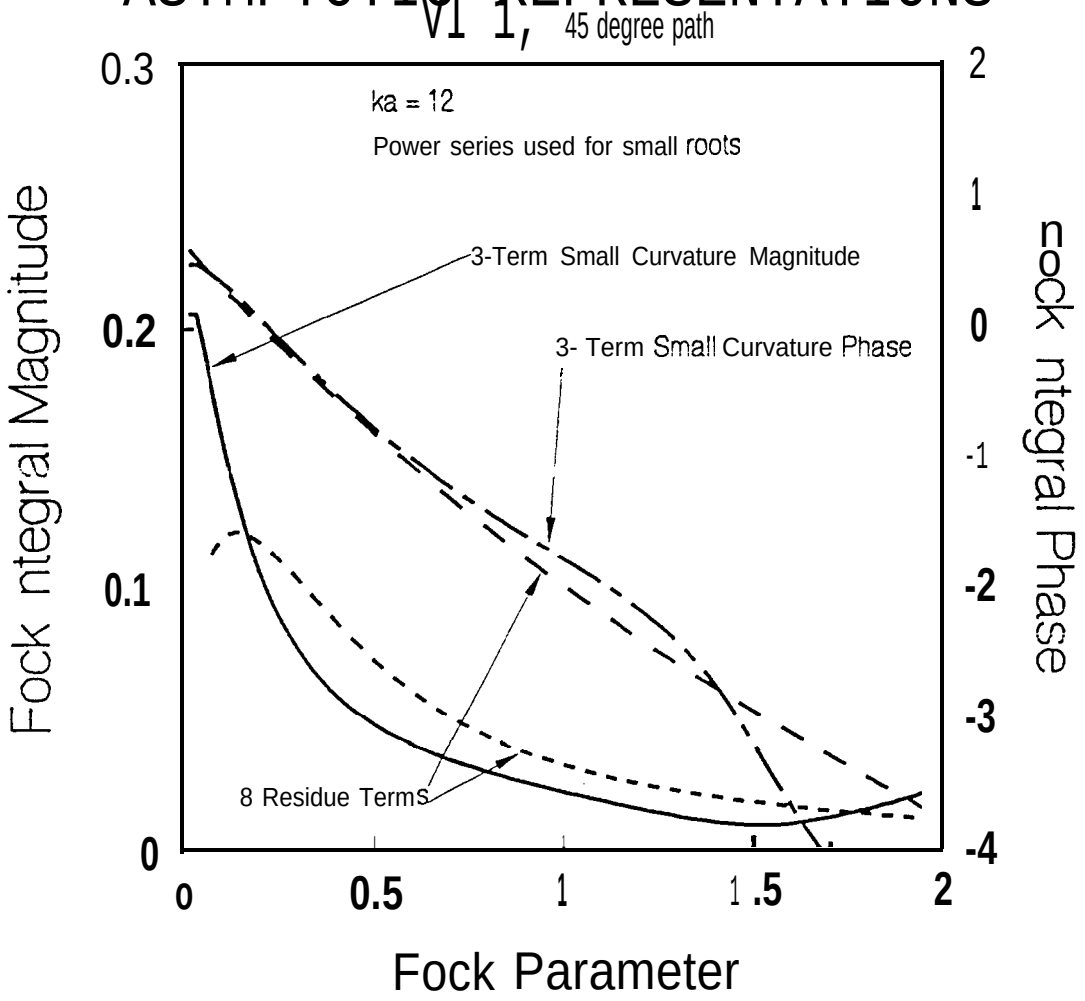

FIG. 10a

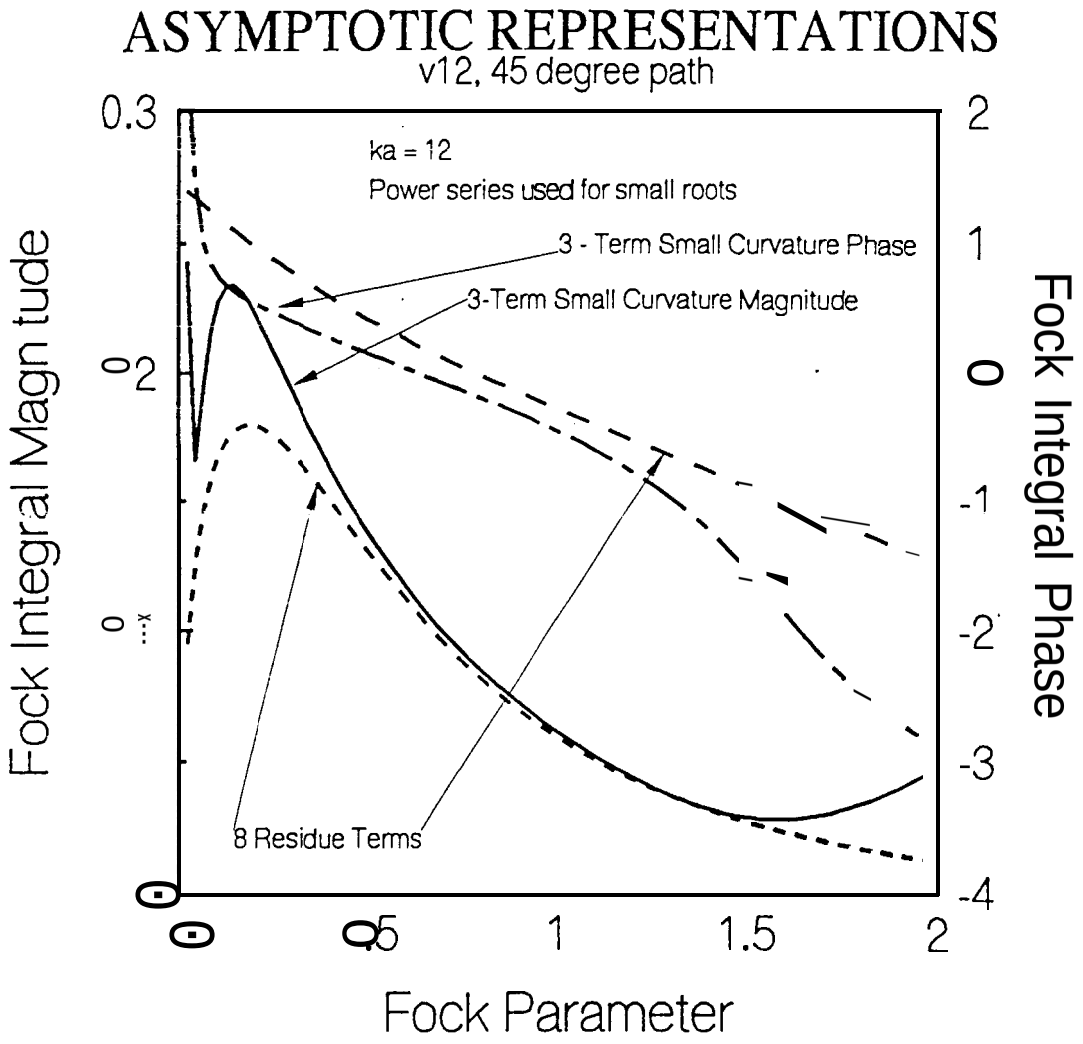
ASYMPTOTIC REPRESENTATIONS
v12, 45 degree path
ka = 12
Power series used for small roots
3 - Term Small Curvature Phase
3-Term Small Curvature Magnitude
8 Residue Terms
Fock Integral Magn tude
Fock Integral Phase
Fock Parameter
0.3
0
2
0
...x
0
0.5
1
1.5
2
1
0
-1
-2
-3
-4

FIG. 10b

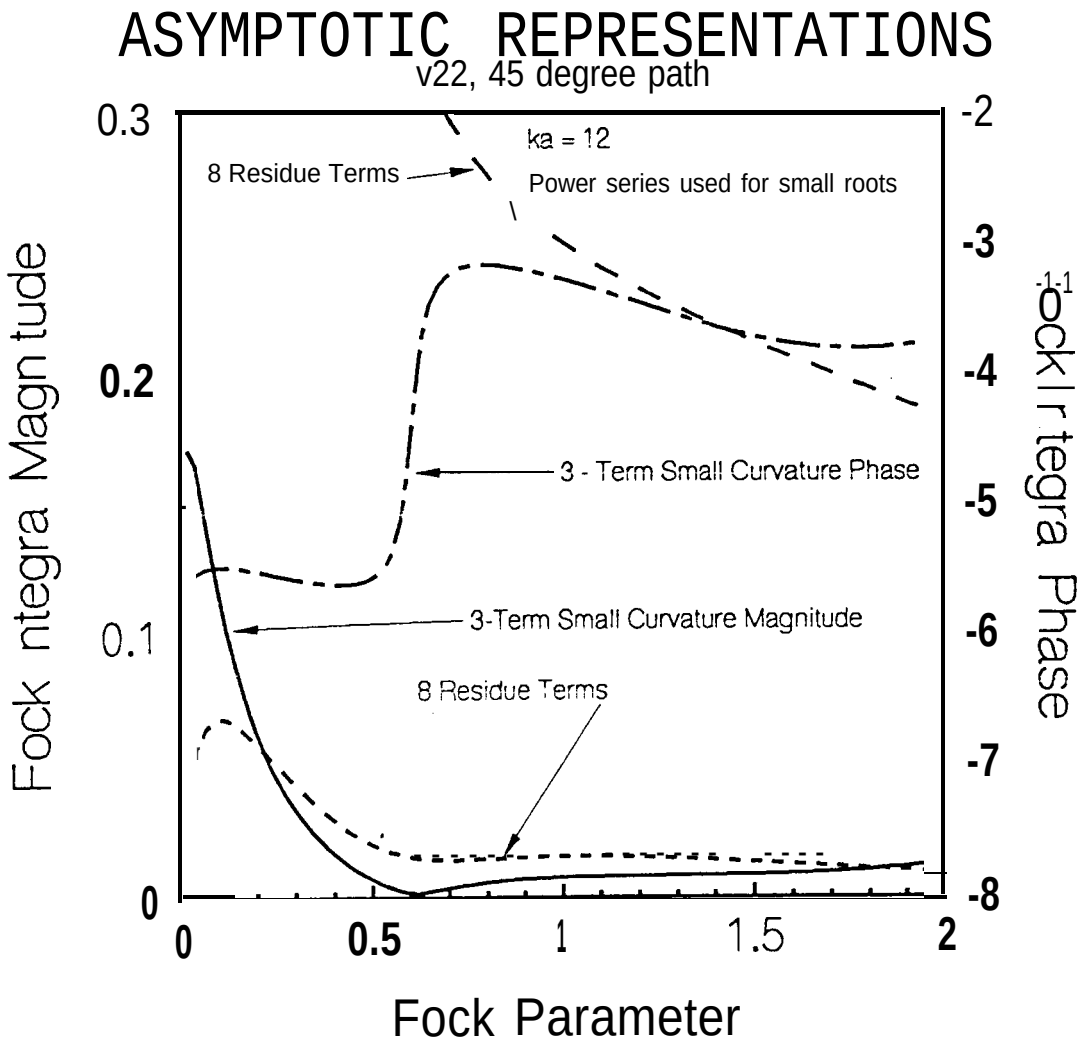
ASYMPTOTIC REPRESENTATIONS
v22, 45 degree path
ka = 12
8 Residue Terms
Power series used for small roots
3 - Term Small Curvature Phase
3-Term Small Curvature Magnitude
8 Residue Terms
Fock ntegra Magn tude
ock I r tegra Phase
Fock Parameter
0.3
0.2
0.1
0
-2
-3
-4
-5
-6
-7
-8
0
0.5
1
1.5
2

FIG. 10c

ASYMPTOTIC REPRESENTATIONS

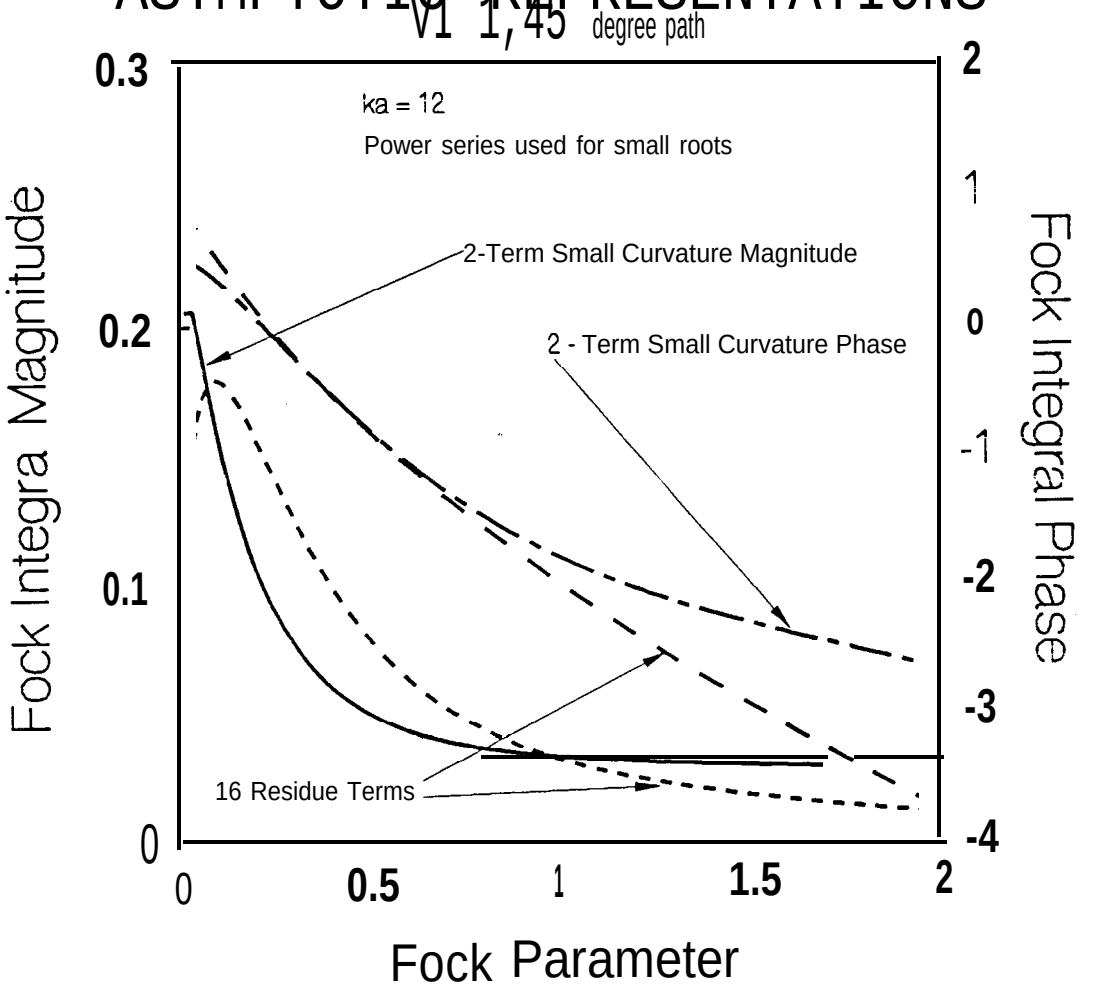

ASYMPTOTIC REPRESENTATIONS VI

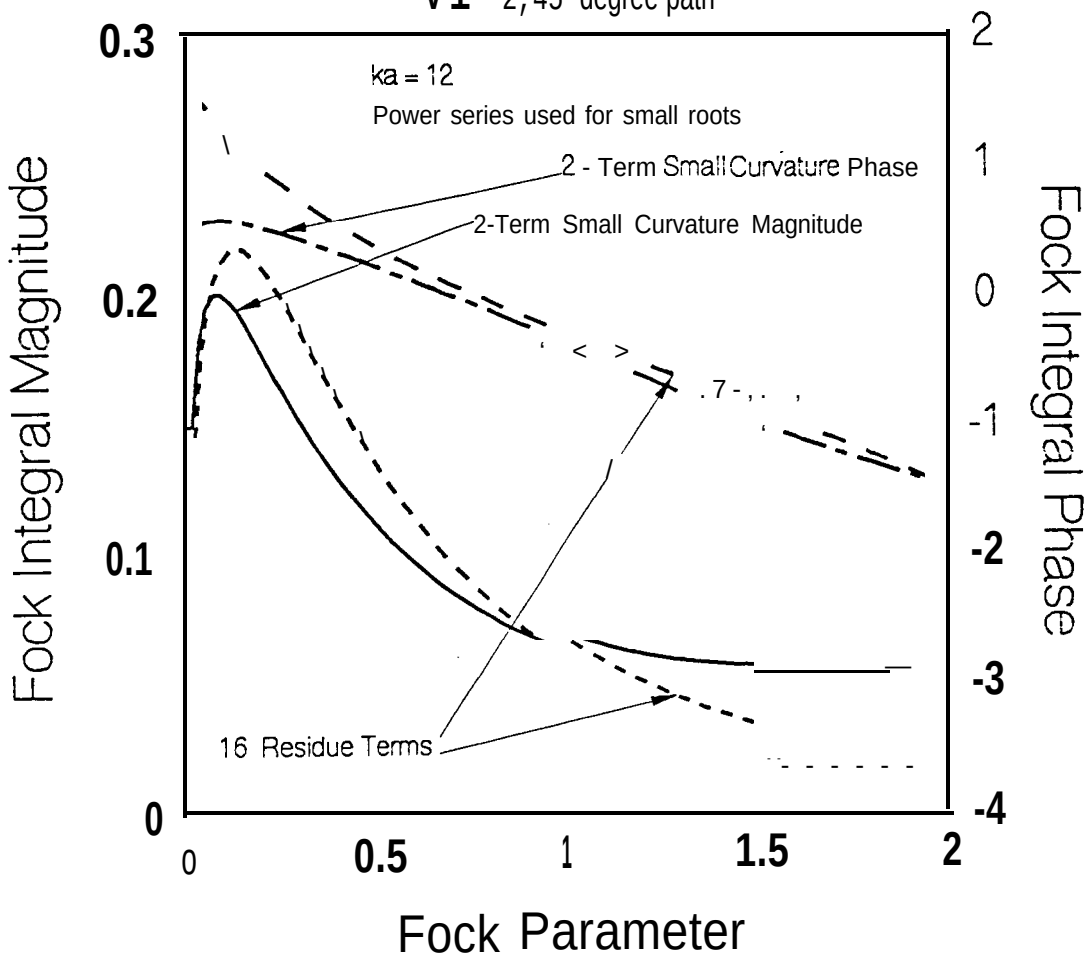

FIG. 116

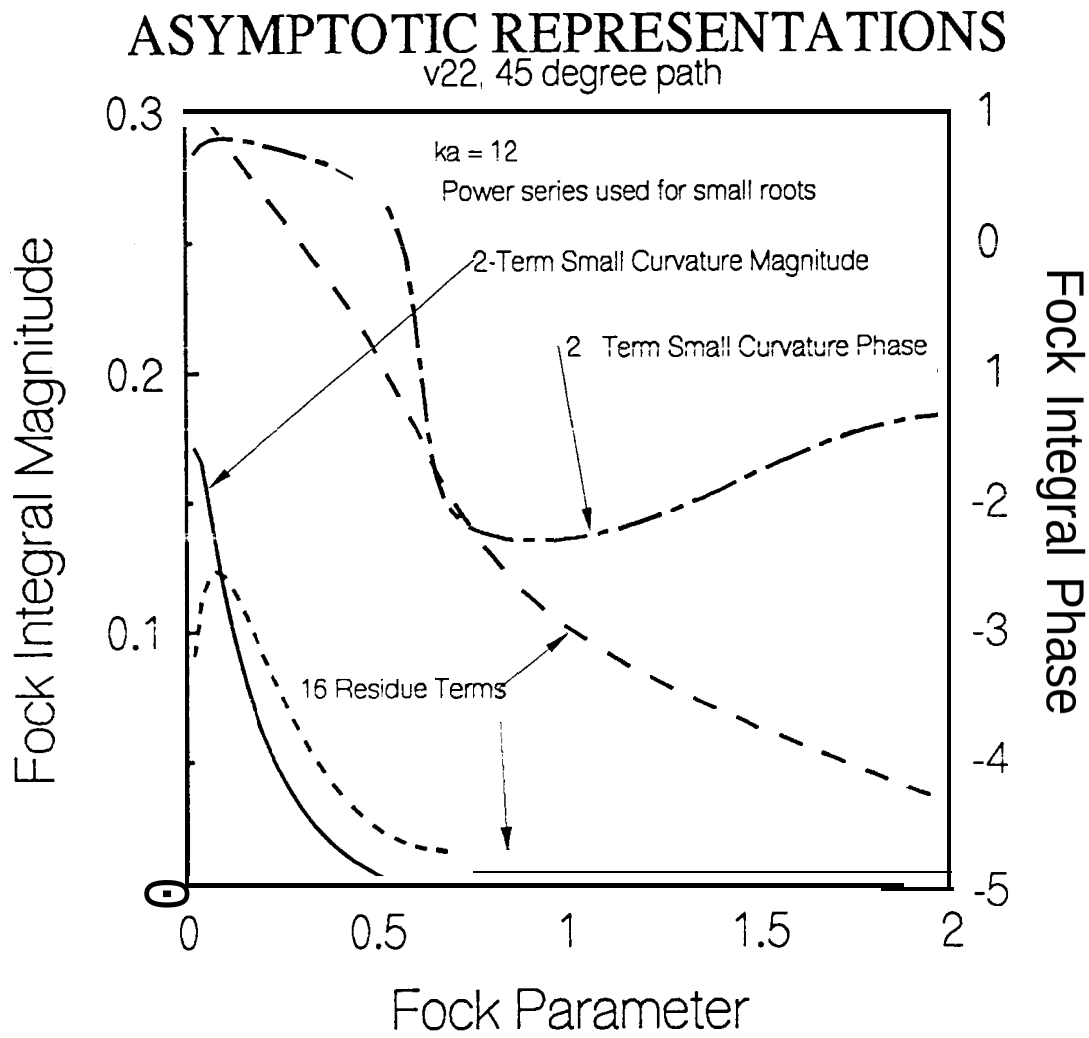
ASYMPTOTIC REPRESENTATIONS
v22, 45 degree path
ka = 12
Power series used for small roots
2-Term Small Curvature Magnitude
2 Term Small Curvature Phase
16 Residue Terms
Fock Integral Magnitude
Fock Integral Phase
Fock Parameter
0.3
0.2
0.1
0
1
0
-1
-2
-3
-4
-5
0
0.5
1
1.5
2

FIG. 11C

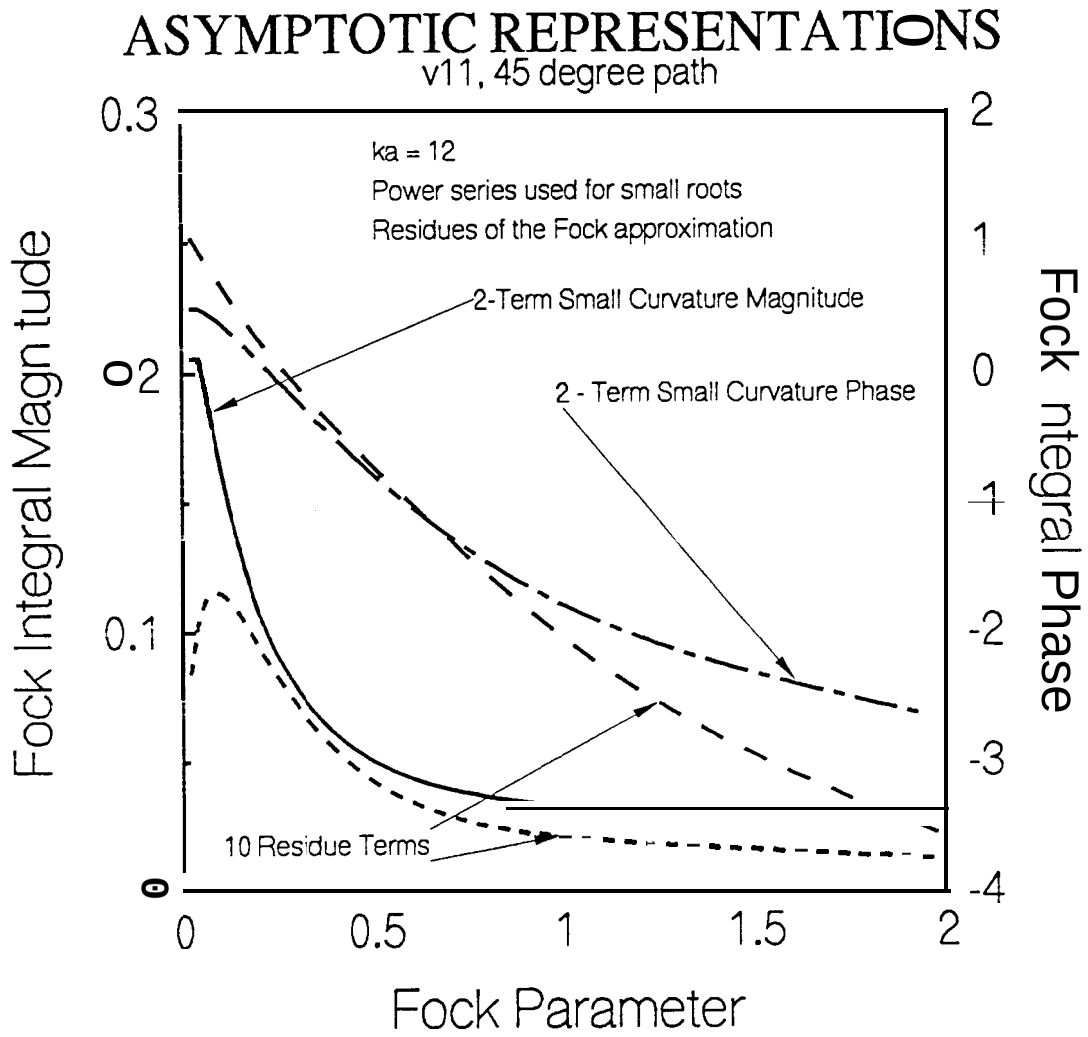
ASYMPTOTIC REPRESENTATIONS
v11, 45 degree path
ka = 12
Power series used for small roots
Residues of the Fock approximation
2-Term Small Curvature Magnitude
2 - Term Small Curvature Phase
10 Residue Terms
Fock Integral Magn tude
Fock ntegral Phase
Fock Parameter
0.3
0.2
0.1
0
2
1
0
-1
-2
-3
-4
0
0.5
1
1.5
2

FIG. 12a

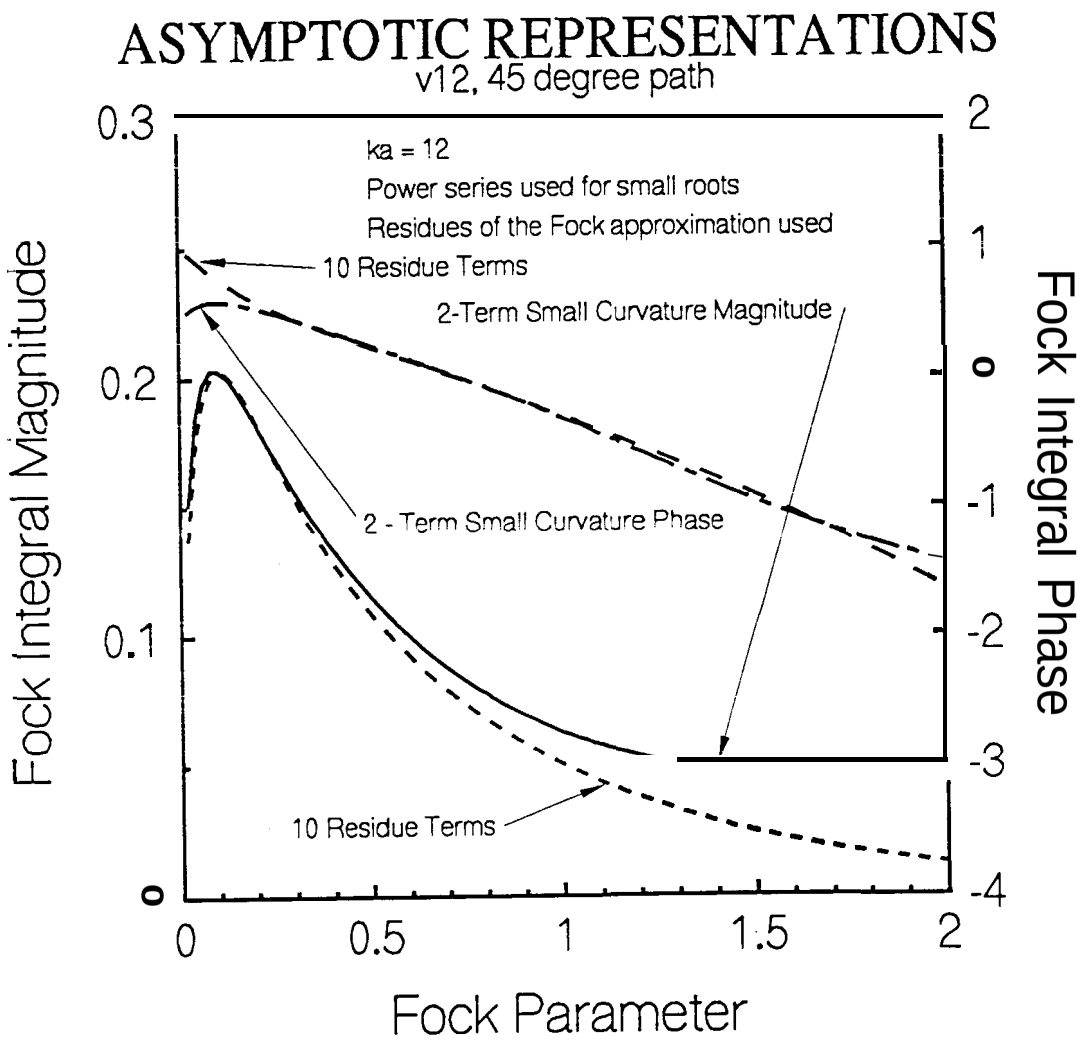
ASYMPTOTIC REPRESENTATIONS
v12, 45 degree path
ka = 12
Power series used for small roots
Residues of the Fock approximation used
10 Residue Terms
2-Term Small Curvature Magnitude
2 - Term Small Curvature Phase
10 Residue Terms
Fock Integral Magnitude
Fock Integral Phase
Fock Parameter
0.3
0.2
0.1
0
2
1
0
-1
-2
-3
-4
0
0.5
1
1.5
2

FIG. 12b

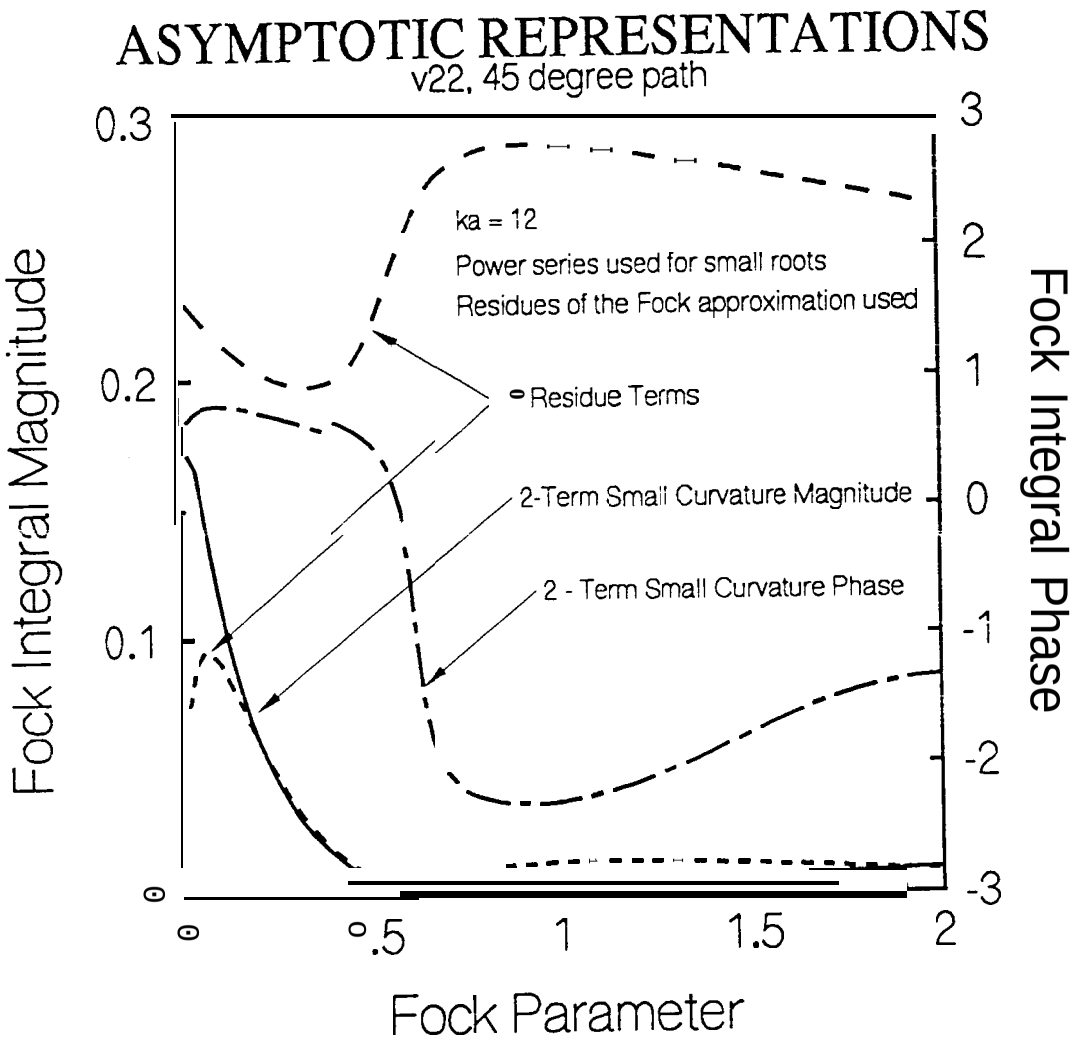
ASYMPTOTIC REPRESENTATIONS
v22, 45 degree path
ka = 12
Power series used for small roots
Residues of the Fock approximation used
Residue Terms
2-Term Small Curvature Magnitude
2 - Term Small Curvature Phase
Fock Integral Magnitude
Fock Integral Phase
Fock Parameter
0.3
0.2
0.1
0
3
2
1
0
-1
-2
-3
0
.5
1
1.5
2

FIG. 12C